

Non-negative Matrix Factorization Algorithms Generally Improve Topic Model Fits

Peter Carbonetto

Department of Human Genetics, University of Chicago, Chicago, IL, 60637*

Abhishek Sarkar

Department of Human Genetics, University of Chicago, Chicago, IL, 60637
and Vesalius Therapeutics, Cambridge, MA, 02142

Zihao Wang

Department of Statistics, University of Chicago, Chicago, IL, 60637
and

Matthew Stephens

Departments of Statistics and Human Genetics
University of Chicago, Chicago, IL, 60637

July 4, 2025

Abstract

In an effort to develop topic modeling methods that can be quickly applied to large data sets, we revisit the problem of maximum-likelihood estimation in topic models. It is known, at least informally, that maximum-likelihood estimation in topic models is closely related to non-negative matrix factorization (NMF). Yet, to our knowledge, this relationship has not been exploited previously to fit topic models. We show that recent advances in NMF optimization methods can be leveraged to fit topic models very efficiently, often resulting in much better fits and in less time than existing algorithms for topic models. We also formally make the connection between the NMF optimization problem and maximum-likelihood estimation for the topic model, and using this result we show that the expectation maximization (EM) algorithm for the topic model is essentially the same as the classic multiplicative updates for NMF (the only difference being that the operations are performed in a different order). Our methods are implemented in the R package **fastTopics**.

Keywords: Topic models, non-negative matrix factorization, nonconvex optimization, expectation maximization, maximum-likelihood estimation

*Corresponding author (pcarbo@uchicago.edu).

1 Introduction

The focus of this paper is the problem of computing maximum-likelihood estimates (MLEs) of the parameters in a topic model given a $n \times m$ matrix of counts [1]. This problem can be expressed as an optimization problem with linear constraints on the variables. (Note that, since finding the global maximum—that is, the MLE—is NP-hard [2], we seek only to find a local maximum of the likelihood.) Instead of solving this optimization problem, we propose to solve a similar problem with much simpler constraints on the parameters: optimizing a non-negative matrix factorization (NMF) based on a Poisson model of the data [3–8]. While several papers have developed formal connections between Poisson NMF and the topic model [9–16], as far as we are aware none have previously suggested using Poisson NMF algorithms for fitting topic models.

Reframing the problem of fitting a topic model as an NMF optimization problem has enabled us and others to efficiently fit topic models to very large single-cell data sets, in some cases with hundreds of thousands of cells and hundreds of thousands genomic features; that is, a counts matrix with more than 100,000 rows and columns [17–28]. (See also [29, 30] for earlier work on applying topic models to single-cell data.) Our approach contrasts with the much more widely used variational inference algorithms for topic models (“latent Dirichlet allocation”) [31–33]. The benefit of variational inference is that it produces approximate posterior estimates of the model parameters, which can help to address overfitting, stabilize the parameter estimation, and increase its accuracy. However, the underlying computations for variational inference are more complex, making the algorithms slower and more challenging to apply to very large data sets. For these reasons, “online” variational inference algorithms have been developed that are much faster and can handle very large data sets [34, 35]. But online learning algorithms have their own challenges; for example, unlike conventional optimization algorithms, they do not guarantee that the objective will improve at each iteration, and the results of online learning are often sensitive to parameter tuning. (Markov chain Monte Carlo algorithms for posterior inference in topic models have also been used in the past [36], but these are even more computationally burdensome than variational inference.) Therefore, on balance, maximum-likelihood estimation remains an attractive option for very large data sets, especially when maximum-likelihood estimation is implemented using very fast NMF algorithms, as we show here.

Prior to LDA and variational inference for the topic model, Hofmann [1] used a simple expectation maximization (EM) algorithm to obtain MLEs under the topic model [1]. However, it is known that in certain settings EM can be very slow to converge to a local maximum of the likelihood [37–43]. The slow convergence of EM is sometimes viewed as a feature, not a bug: stopping an EM or other optimization algorithm early has been shown anecdotally, and in theory, to result in parameter estimates that better generalize performance to test sets; that is, this early stopping can *implicitly regularize* the MLEs [44, 45]. However, we show that this slow convergence can also cause the EM to get “stuck” in areas of the likelihood that are far away from a local maximum. We show that NMF algorithms can very quickly “rescue” the EM estimates, resulting in parameter estimates

that are very different from and much better than the estimates produced by EM.

A key intuition for this approach is that the Poisson NMF optimization problem is simpler than the topic model optimization problem because it lacks the “sum-to-one” constraints. However, not all Poisson NMF algorithms exploit this benefit. Indeed, the traditional way to solve Poisson NMF—the “multiplicative updates” of [4]—is equivalent to EM [46], and is closely related to the EM algorithms traditionally used to fit topic models. Therefore, the Poisson NMF multiplicative updates are expected to experience the same slow convergence issues as EM, and this is indeed borne out by our empirical results. In contrast, other recently developed algorithms for solving Poisson NMF based on co-ordinate descent (CD) [47, 48] do not have an existing counterpart in the topic model literature. (Consider that co-ordinate descent cannot obviously deal with the sum-to-one constraints.) These CD algorithms can greatly outperform the multiplicative updates for Poisson NMF [8], and in this paper we also show that these algorithms yield substantial performance gains for fitting topic models.

The algorithms for topic models and Poisson NMF described in this paper are implemented in an R package, `fastTopics`, available on CRAN (<https://cran.r-project.org/package=fastTopics>) and GitHub (<https://github.com/stephenslab/fastTopics/>).

2 Poisson NMF and the Multinomial Topic Model

In the following, we provide side-by-side descriptions of the topic model and Poisson NMF to highlight their close connection. While formal and informal connections between these two models have been made previously [9–14, 16], these previous papers draw connections between the algorithms and/or stationary points of the objective functions. Here we state a simple and more general result relating the likelihoods of the two models (Lemma 1), which we view as a more fundamental result underlying previous results.¹

Let $\mathbf{X} \in \mathbf{R}_+^{n \times m}$ denote an $n \times m$ matrix of observed counts x_{ij} . For example, when analyzing text documents, n is the number of documents, m is the number of unique terms, and x_{ij} is the number of times term j occurs in document i . Both Poisson NMF and the topic model can be seen as fitting different—but closely related—models of \mathbf{X} .

The Poisson NMF model has parameters that are non-negative matrices, $\mathbf{H} \in \mathbf{R}_+^{n \times K}$ and $\mathbf{W} \in \mathbf{R}_+^{m \times K}$, where $\mathbf{R}_+^{r \times c}$ denotes the set of non-negative, real matrices with r rows and c columns. Given a $K \geq 1$, the Poisson NMF model is

$$\begin{aligned} x_{ij} \mid \mathbf{H}, \mathbf{W} &\sim \text{Poisson}(\lambda_{ij}) \\ \lambda_{ij} &= (\mathbf{H}\mathbf{W}^T)_{ij} = \sum_{k=1}^K h_{ik}w_{jk}, \end{aligned} \tag{1}$$

where h_{ik}, w_{jk} denote elements of matrices \mathbf{H}, \mathbf{W} . Poisson NMF can be viewed as a rank- K matrix factorization by noting that (1) implies $E[\mathbf{X}] = \mathbf{H}\mathbf{W}^T$, so fitting a Poisson NMF

¹Recent papers have also studied the problem of identifying “anchor words,” which are words that appear in exactly one topic. In this setting, there is also a close relationship between the algorithms for identifying anchor words and the algorithms for identifying “separable” non-negative factors [2, 15, 49–51].

essentially seeks values of \mathbf{H} and \mathbf{W} such that $\mathbf{X} \approx \mathbf{H}\mathbf{W}^T$.² Computing an MLE for the Poisson NMF model reduces to the following bound-constrained optimization problem:

$$\begin{aligned} & \text{minimize} && \ell(\mathbf{X}; \mathbf{H}, \mathbf{W}) \\ & \text{subject to} && \mathbf{H} \geq \mathbf{0}, \mathbf{W} \geq \mathbf{0}, \end{aligned} \quad (2)$$

in which the objective function is

$$\ell(\mathbf{X}; \mathbf{H}, \mathbf{W}) = \phi(\mathbf{X}; \mathbf{H}, \mathbf{W}) + \|\mathbf{H}\mathbf{W}^T\|_{1,1}, \quad (3)$$

where $\|\mathbf{A}\|_{1,1} = \sum_{i=1}^n \sum_{j=1}^m |a_{ij}|$ is the $L_{1,1}$ norm of $n \times m$ matrix \mathbf{A} .

While there have been many different approaches to topic modeling, with different fitting procedures and different prior distributions—examples include the aspect model [54], probabilistic latent semantic indexing [1, 34, 55] and latent Dirichlet allocation [31]—most of these approaches are based on the same basic model: a multinomial distribution of the counts. We therefore refer to this model as the *multinomial topic model*. Like Poisson NMF, the multinomial topic model is also parameterized by two non-negative matrices, $\mathbf{L} \in \mathbf{R}_+^{n \times K}$, $\mathbf{F} \in \mathbf{R}_+^{m \times K}$, but the elements of these two matrices must satisfy additional “sum-to-one” constraints:

$$\sum_{j=1}^m f_{jk} = 1, \quad \sum_{k=1}^K l_{ik} = 1. \quad (4)$$

Given a $K \geq 2$, the multinomial topic model is

$$\begin{aligned} x_{i1}, \dots, x_{im} \mid \mathbf{L}, \mathbf{F}, t_i &\sim \text{Multinom}(t_i; \pi_{i1}, \dots, \pi_{im}) \\ \pi_{ij} &= (\mathbf{L}\mathbf{F}^T)_{ij} = \sum_{k=1}^K l_{ik} f_{jk}, \end{aligned} \quad (5)$$

in which $t_i := \sum_{j=1}^m x_{ij}$. The multinomial topic model is also a matrix factorization because we have that $\mathbf{\Pi} = \mathbf{L}\mathbf{F}^T$, where $\mathbf{\Pi}$ denotes the matrix of multinomial probabilities π_{ij} [1, 56, 57]. Computing an MLE for the multinomial topic model reduces to the following linearly-constrained optimization problem:

$$\begin{aligned} & \text{minimize} && \phi(\mathbf{X}; \mathbf{L}, \mathbf{F}) \\ & \text{subject to} && \mathbf{L}\mathbf{1}_K = \mathbf{1}_n \\ & && \mathbf{F}^T\mathbf{1}_m = \mathbf{1}_K \\ & && \mathbf{L} \geq \mathbf{0}, \mathbf{F} \geq \mathbf{0}, \end{aligned} \quad (6)$$

in which $\mathbf{1}_d = (1, \dots, 1)^T$ denotes a column vector of ones of length d , and the objective function is

$$\phi(\mathbf{L}, \mathbf{F}) = - \sum_{i=1}^n \sum_{j=1}^m x_{ij} \log l_i^T \mathbf{f}_j, \quad (7)$$

²In descriptions of NMF, it is more common to represent data vectors (e.g., documents) as *columns* of \mathbf{X} (e.g., [4, 15, 52]), in which case one would write $\mathbf{X} \approx \mathbf{W}\mathbf{H}^T$. Here, we represent documents as *rows* of \mathbf{X} , following for example [1, 53]. Due to the symmetry of Poisson NMF (1), it makes no difference if we fit $\mathbf{X} \approx \mathbf{H}\mathbf{W}^T$ or $\mathbf{X}^T \approx \mathbf{H}\mathbf{W}^T$. It only matters when connecting Poisson NMF to the topic model.

where $\mathbf{l}_i, \mathbf{f}_j$ denote, respectively, the i th row of \mathbf{L} and the j th row of \mathbf{F} .

Now we connect the Poisson non-negative matrix factorization with parameters \mathbf{H}, \mathbf{W} to the multinomial topic model matrix factorization with parameters \mathbf{L}, \mathbf{F} . To do so, we define a mapping between the parameter spaces for the two models (Definition 1), then we state an equivalence between their likelihoods (Lemma 1), which leads to an equivalence in their MLEs (Corollary 1).

Definition 1 (Poisson NMF to multinomial topic model reparameterization). Let \mathbf{R}_{++}^d denote the set of positive real vectors of length d , let $\mathbf{R}_{\text{row}}^{r \times c}$ denote the set of $r \times c$ row-normalized matrices (non-negative matrices \mathbf{A} with the property that the elements in each row of \mathbf{A} sum to 1), and let $\mathbf{R}_{\text{col}}^{r \times c}$ denote the set of $r \times c$ column-normalized matrices (non-negative matrices \mathbf{A} with the property that the elements in each column of \mathbf{A} sum to 1). For $K \geq 2$, $\mathbf{H} \in \mathbf{R}_{++}^{n \times K}$, $\mathbf{W} \in \mathbf{R}_{++}^{m \times K}$, define mapping $\text{PNMF-TO-MTM} : \mathbf{H}, \mathbf{W} \mapsto \mathbf{L}, \mathbf{F}, \mathbf{s}, \mathbf{u}$, with $\mathbf{L} \in \mathbf{R}_{\text{row}}^{n \times K}$, $\mathbf{F} \in \mathbf{R}_{\text{col}}^{m \times K}$, $\mathbf{s} \in \mathbf{R}_{++}^n$, $\mathbf{u} \in \mathbf{R}_{++}^K$ by the following procedure:

PNMF-TO-MTM(\mathbf{H}, \mathbf{W})

- 1 $\mathbf{F}, \mathbf{u} \leftarrow \text{NORMALIZE-COLS}(\mathbf{W})$
- 2 $\mathbf{U} \leftarrow \text{diag}(\mathbf{u})$
- 3 $\mathbf{L}, \mathbf{s} \leftarrow \text{NORMALIZE-ROWS}(\mathbf{H}\mathbf{U})$
- 4 **return** ($\mathbf{L}, \mathbf{F}, \mathbf{s}, \mathbf{u}$)

This procedure has two subroutines, defined as follows: **NORMALIZE-ROWS**(\mathbf{A}) returns a vector $\mathbf{y} \in \mathbf{R}_{++}^r$ containing the row sums of $r \times c$ matrix \mathbf{A} , $y_i = \sum_{j=1}^c a_{ij}$, and $\mathbf{B} \in \mathbf{R}_{\text{row}}^{r \times c}$, a row-normalized matrix with entries $b_{ij} = a_{ij}/y_i$; **NORMALIZE-COLS**(\mathbf{A}) returns a vector $\mathbf{y} \in \mathbf{R}_{++}^c$ containing the column sums of \mathbf{A} , $y_j = \sum_{i=1}^r a_{ij}$, and $\mathbf{B} \in \mathbf{R}_{\text{col}}^{r \times c}$, a column-normalized matrix with entries $b_{ij} = a_{ij}/y_j$. We also define $\text{diag}(\mathbf{a})$ as the $n \times n$ diagonal matrix \mathbf{A} with diagonal entries given by the elements of vector \mathbf{a} .

NORMALIZE-ROWS also defines a mapping **NORMALIZE-ROWS** : $\mathbf{A} \mapsto \mathbf{B}, \mathbf{y}$, with $\mathbf{A} \in \mathbf{R}_{++}^{r \times c}$, $\mathbf{B} \in \mathbf{R}_{\text{row}}^{r \times c}$, $\mathbf{y} \in \mathbf{R}_{++}^r$. If each row of \mathbf{A} has at least one positive element, then this mapping is one-to-one, and therefore, **NORMALIZE-ROWS** defines a *change of variables* from non-negative matrices \mathbf{A} to row-normalized matrices \mathbf{B} and positive vectors \mathbf{y} . Similarly, **NORMALIZE-COLS** : $\mathbf{A} \mapsto \mathbf{B}, \mathbf{y}$ defines a change of variables from non-negative matrices \mathbf{A} to column-normalized matrices \mathbf{B} and positive vectors \mathbf{y} (provided that each column of \mathbf{A} has at least one positive element). These together imply that **MTM-TO-PNMF** defines a change of variables from non-negative matrices \mathbf{H}, \mathbf{W} to positive vectors \mathbf{s}, \mathbf{u} , row-normalized matrices \mathbf{L} , and column-normalized matrices \mathbf{F} . The \mathbf{F} and \mathbf{L} satisfy the sum-to-one constraints (4). The inverse mapping, **MTM-TO-PNMF** := **PNMF-TO-MTM**⁻¹ : $\mathbf{L}, \mathbf{F}, \mathbf{s}, \mathbf{u} \mapsto \mathbf{H}, \mathbf{W}$, is $\mathbf{W} \leftarrow \mathbf{F}\mathbf{U}$, $\mathbf{H} \leftarrow \mathbf{S}\mathbf{L}\mathbf{U}^{-1}$, where $\mathbf{U} := \text{diag}(\mathbf{u})$, $\mathbf{S} := \text{diag}(\mathbf{s})$.

Lemma 1 (Equivalence of Poisson NMF and multinomial topic model likelihoods). Denote the Poisson NMF model probability density by $p_{\text{PNMF}}(\mathbf{X} \mid \mathbf{H}, \mathbf{W})$ and denote the multinomial topic model probability density by $p_{\text{MTM}}(\mathbf{X} \mid \mathbf{L}, \mathbf{F})$. Assume $\mathbf{H} \in \mathbf{R}_{++}^{n \times K}$ and $\mathbf{W} \in \mathbf{R}_{++}^{m \times K}$, define $t_i := \sum_{j=1}^m x_{ij}$, and let $\mathbf{L}, \mathbf{F}, \mathbf{s}, \mathbf{u}$ be the result of applying **PNMF-TO-MTM** to \mathbf{H}, \mathbf{W} .

Then we have that

$$p_{\text{PNMF}}(\mathbf{X} \mid \mathbf{H}, \mathbf{W}) = p_{\text{MTM}}(\mathbf{X} \mid \mathbf{L}, \mathbf{F}) \times \prod_{i=1}^n \text{Poisson}(t_i; s_i). \quad (8)$$

Proof. The result is obtained by applying the following identity relating the multinomial and Poisson distributions [58, 59]:

$$\prod_{j=1}^m \text{Poisson}(x_j; \lambda_j) = \text{Multinom}(\mathbf{x}; t, \lambda_1/s, \dots, \lambda_m/s) \times \text{Poisson}(t; s), \quad (9)$$

such that $\mathbf{x} = (x_1, \dots, x_m)$, $\lambda_1, \dots, \lambda_m \in \mathbf{R}_+$, $s := \sum_{j=1}^m \lambda_j$ and $t := \sum_{j=1}^m x_j$. \square

Now we use this lemma to provide justification for solving the Poisson NMF optimization problem in order to compute an MLE for the multinomial topic model. First, consider an augmented form of the multinomial topic model optimization problem:

$$\begin{aligned} & \text{minimize} && \phi_{\text{aug}}(\mathbf{X}; \mathbf{L}, \mathbf{F}, \mathbf{s}) \\ & \text{subject to} && \mathbf{L} \mathbf{1}_K = \mathbf{1}_n \\ & && \mathbf{F}^T \mathbf{1}_m = \mathbf{1}_K \\ & && \mathbf{L} \geq \mathbf{0}, \mathbf{F} \geq \mathbf{0}, \mathbf{s} \geq \mathbf{0}, \end{aligned} \quad (10)$$

in which the augmented objective is

$$\phi_{\text{aug}}(\mathbf{X}; \mathbf{L}, \mathbf{F}) = \phi(\mathbf{X}; \mathbf{L}, \mathbf{F}) + \psi(\mathbf{X}; \mathbf{s}) \quad (11)$$

$$\psi(\mathbf{X}; \mathbf{s}) = \sum_{i=1}^n s_i - \sum_{i=1}^n \sum_{j=1}^m x_{ij} \log s_i. \quad (12)$$

Notice that solutions to (10) are also solutions to (6) because the objective and constraints for the \mathbf{L}, \mathbf{F} have not changed. The Poisson NMF objective $\ell(\mathbf{X}; \mathbf{H}, \mathbf{W})$ is equal to the Poisson log-likelihood, $\log p_{\text{PNMF}}(\mathbf{X} \mid \mathbf{H}, \mathbf{W})$ (ignoring constant terms), and the multinomial topic model augmented objective $\phi_{\text{aug}}(\mathbf{X}; \mathbf{L}, \mathbf{F}, \mathbf{s})$ is equal to the logarithm of the right-hand side of (8) (ignoring constant terms). This means that any optimization algorithm that improves the Poisson NMF objective $\ell(\mathbf{X}; \mathbf{H}, \mathbf{W})$ will also improve the augmented objective $\phi_{\text{aug}}(\mathbf{X}; \mathbf{L}, \mathbf{F}, \mathbf{s})$ so long as PNMF-TO-MTM is used to recover $\mathbf{L}, \mathbf{F}, \mathbf{s}$ from \mathbf{H}, \mathbf{W} . We formalize the relationship between the two optimization problems in the following corollary.

Corollary 1 (Relationship between MLEs for Poisson NMF and multinomial topic model). Let $\hat{\mathbf{H}} \in \mathbf{R}_+^{n \times K}$, $\hat{\mathbf{W}} \in \mathbf{R}_+^{m \times K}$ denote MLEs for the Poisson NMF model,³

$$\hat{\mathbf{H}}, \hat{\mathbf{W}} \in \underset{\mathbf{H} \in \mathbf{R}_+^{n \times K}, \mathbf{W} \in \mathbf{R}_+^{m \times K}}{\text{argmax}} p_{\text{PNMF}}(\mathbf{X} \mid \mathbf{H}, \mathbf{W}). \quad (13)$$

Equivalently, $\hat{\mathbf{H}}, \hat{\mathbf{W}}$ can be defined as a solution to (2). If $\hat{\mathbf{L}}, \hat{\mathbf{F}}$ are obtained by applying PNMF-TO-MTM to $\hat{\mathbf{H}}, \hat{\mathbf{W}}$ (Definition 1), then these are also MLEs for the multinomial topic model,

$$\hat{\mathbf{L}}, \hat{\mathbf{F}} \in \underset{\mathbf{L} \in \mathbf{R}_{\text{row}}^{n \times K}, \mathbf{F} \in \mathbf{R}_{\text{col}}^{n \times K}}{\text{argmax}} p_{\text{MTM}}(\mathbf{X} \mid \mathbf{L}, \mathbf{F}). \quad (14)$$

³The notation $\hat{\theta} \in \text{argmax}_{\theta} f(\theta)$ means $f(\hat{\theta}) \geq f(\theta)$ for all θ , and accounts for the fact that an MLE may not be unique due to non-identifiability.

(Equivalently, $\hat{\mathbf{L}}, \hat{\mathbf{F}}$ are a solution to eq. 6.)

Conversely, let $\hat{\mathbf{L}} \in \mathbf{R}_{\text{row}}^{n \times K}, \hat{\mathbf{F}} \in \mathbf{R}_{\text{col}}^{m \times K}$ denote multinomial topic model MLEs, set $\hat{\mathbf{s}} = \mathbf{t} := (t_1, \dots, t_n)$, and choose any $\hat{\mathbf{u}} \in \mathbf{R}_{++}^K$. If $\hat{\mathbf{H}}, \hat{\mathbf{W}}$ are obtained by applying MTM-TO-PNMF to $\hat{\mathbf{L}}, \hat{\mathbf{F}}, \hat{\mathbf{s}}, \hat{\mathbf{u}}$ (see Definition 1), these are also Poisson NMF MLEs (13).

Proof. We prove this result using “equivalent optimization problems” [60]. Since PNMF-TO-MTM defines a change of variables, we can apply the change of variables to (10) to obtain an equivalent optimization problem with optimization variables \mathbf{H}, \mathbf{W} ,

$$\begin{aligned} & \text{minimize} && \phi_{\text{aug}}(\mathbf{X}; \text{PNMF-TO-MTM}(\mathbf{H}, \mathbf{W})) \\ & \text{subject to} && \mathbf{H} \geq \mathbf{0}, \mathbf{W} \geq \mathbf{0}, \end{aligned} \quad (15)$$

in which the \mathbf{u} returned by PNMF-TO-MTM is ignored. From Lemma 1, we can rewrite (15) as

$$\begin{aligned} & \text{minimize} && \ell(\mathbf{X}; \mathbf{H}, \mathbf{W}) + \text{const} \\ & \text{subject to} && \mathbf{H} \geq \mathbf{0}, \mathbf{W} \geq \mathbf{0}, \end{aligned} \quad (16)$$

which is exactly the Poisson NMF optimization problem (ignoring terms that do not depend on \mathbf{H} or \mathbf{W}). Therefore, the augmented optimization problem (10) and the Poisson NMF optimization problem (2) are related to each other by the change of variables $\text{PNMF-TO-MTM}(\mathbf{H}, \mathbf{W}) = (\mathbf{L}, \mathbf{F}, \mathbf{s}, \mathbf{u})$. Since solutions to the augmented optimization problem (10) are also solutions to the original problem (6), it follows that Poisson NMF MLEs $\hat{\mathbf{H}}, \hat{\mathbf{W}}$ recover multinomial topic model MLEs $\hat{\mathbf{L}}, \hat{\mathbf{F}}$. The reverse—that multinomial topic model MLEs $\hat{\mathbf{L}}, \hat{\mathbf{F}}$ recover Poisson NMF MLEs $\hat{\mathbf{H}}, \hat{\mathbf{W}}$ —requires the additional step of solving $\hat{\mathbf{s}} := \arg\min_{\mathbf{s} \in \mathbf{R}_{++}^n} \psi(\mathbf{s}) = \arg\max_{\mathbf{s} \in \mathbf{R}_{++}^n} \prod_{i=1}^n \text{Poisson}(t_i; s_i)$, which has unique solution $\hat{\mathbf{s}} = \mathbf{t}$ provided that $t_1, \dots, t_n > 0$. \square

Remark. Since \mathbf{H}, \mathbf{W} are not uniquely identifiable—for example, multiplying the k th column of \mathbf{H} by $a_k \neq 0$ and dividing the k th column of \mathbf{W} by a_k does not change $\mathbf{H}\mathbf{W}^T$ —one way to avoid this non-identifiability is to impose constraints or penalty terms to the objective. However, introducing constraints or penalties on \mathbf{H}, \mathbf{W} (or \mathbf{L}, \mathbf{F}) may break the above equivalence. We note one form of penalized objective that preserves the equivalence:

$$\phi^*(\mathbf{X}; \mathbf{L}, \mathbf{F}) := \phi(\mathbf{X}; \mathbf{L}, \mathbf{F}) + \rho^{\text{MTM}}(\mathbf{F}), \quad (17)$$

where

$$\rho^{\text{MTM}}(\mathbf{F}) := - \sum_{j=1}^m \sum_{k=1}^K (a_{jk} - 1) \log f_{jk}, \quad (18)$$

and $a_{jk} > 1, j = 1, \dots, m, k = 1, \dots, K$. The equivalent penalized objective for Poisson NMF is

$$\ell^*(\mathbf{X}; \mathbf{H}, \mathbf{W}) := \ell(\mathbf{X}; \mathbf{H}, \mathbf{W}) + \rho^{\text{PNMF}}(\mathbf{W}), \quad (19)$$

where

$$\rho^{\text{PNMF}}(\mathbf{W}) := - \sum_{j=1}^m \sum_{k=1}^K (a_{jk} - 1) \log w_{jk} + \sum_{j=1}^m \sum_{k=1}^K b_k w_{jk}, \quad (20)$$

and $b_k > 0$, $k = 1, \dots, K$. The a_{jk}, b_k are parameters controlling the shape and strength of these penalties. (Setting $a_{jk} = 1, b_k = 0$ recovers the unpenalized objectives.) Minimizing $\phi^*(\mathbf{X}; \mathbf{L}, \mathbf{F})$ corresponds to MAP estimation of \mathbf{L}, \mathbf{F} with Dirichlet priors on \mathbf{F} and uniform priors on \mathbf{L} [61], and minimizing $\ell^*(\mathbf{X}; \mathbf{H}, \mathbf{W})$ corresponds to MAP estimation of \mathbf{W}, \mathbf{H} with gamma priors on \mathbf{W} and uniform priors on \mathbf{H} [11, 46, 62]. The equivalence of MAP estimation with these specific priors generalizes Corollary 1; see Appendix A.

Lemma 1 and Corollary 1 are more general than previous results [10, 12, 14, 15] because they apply to *any* $\mathbf{H}, \mathbf{W}, \mathbf{L}, \mathbf{F}$ from Definition 1, not only a fixed point of the likelihood or objective. See [9, 13, 16] for other related results.

In short, Lemma 1 tells us that Poisson NMF and the multinomial topic model are Poisson and multinomial formulations of the same matrix factorization method. In particular, the shared ability of Poisson NMF and the multinomial topic model to recover a decomposition into “parts” or “topics” is suggested these formal connections.

Although Poisson NMF and the multinomial topic model achieve similar ends—and are identical for maximum-likelihood estimation and some forms of MAP estimation—the two methods still possess different advantages: Poisson NMF has an advantage in computation because it avoids the sum-to-one constraints, whereas the multinomial topic model has the advantage in interpretation because the f_{jk}, l_{ik} can be compared across topics k whereas the Poisson NMF parameters h_{ik}, w_{jk} cannot due to the undetermined column-scaling \mathbf{u} . Therefore, by switching between the two models, we can have the advantages of both.

3 Poisson NMF Algorithms

Corollary 1 implies that *any algorithm for maximum-likelihood estimation in Poisson NMF is also an algorithm for maximum-likelihood estimation in the multinomial topic model*. (This also means that the NP-hardness [2, 63] of the two problems is related.) Fitting the Poisson NMF model involves solving (2), which we restate here in a slightly different way:

$$\begin{aligned} \text{minimize} \quad & \ell(\mathbf{X}; \mathbf{H}, \mathbf{W}) = \sum_{i=1}^n \sum_{j=1}^m \mathbf{h}_i^T \mathbf{w}_j - x_{ij} \log(\mathbf{h}_i^T \mathbf{w}_j) \\ \text{subject to} \quad & \mathbf{H} \geq \mathbf{0}, \mathbf{W} \geq \mathbf{0}, \end{aligned} \tag{21}$$

Here, \mathbf{h}_i and \mathbf{w}_j denote column vectors containing, respectively, the i th row of \mathbf{H} and the j th row of \mathbf{W} , and we assume $K \geq 2$.

To facilitate comparisons of different algorithms for solving (21), in the next section we introduce an “Alternating Poisson Regression” framework for solving (21), then we describe the algorithms we have implemented, drawing on recent work and our own experimentation. See also [8] for a detailed comparison of Poisson NMF algorithms.

3.1 Alternating Poisson Regression for Poisson NMF

Alternating Poisson Regression arises from solving (21) by alternating between optimizing over \mathbf{H} with \mathbf{W} fixed, and optimizing over \mathbf{W} with \mathbf{H} fixed. This is an example of a

Require: $\mathbf{X} \in \mathbf{R}_+^{n \times m}$, initial estimates $\mathbf{H}^{(0)} \in \mathbf{R}_+^{n \times K}$, $\mathbf{W}^{(0)} \in \mathbf{R}_+^{m \times K}$,
and a function FIT-POIS-REG(\mathbf{A}, \mathbf{y}) that returns an MLE of \mathbf{b} in (23).
for $t = 1, 2, \dots$ **do**
 for $i = 1, \dots, n$ **do** {can be performed in parallel}
 $\mathbf{h}_i \leftarrow \text{FIT-POIS-REG}(\mathbf{W}^{(t-1)}, \mathbf{x}_i)$
 Store \mathbf{h}_i in i th row of $\mathbf{H}^{(t)}$
 end for
 for $j = 1, \dots, m$ **do** {can be performed in parallel}
 $\mathbf{w}_j \leftarrow \text{FIT-POIS-REG}(\mathbf{H}^{(t)}, \mathbf{x}_j)$
 Store \mathbf{w}_j in j th row of $\mathbf{W}^{(t)}$
 end for
end for
return $\mathbf{H}^{(t)}, \mathbf{W}^{(t)}$

Algorithm 1: Alternating Poisson Regression for Poisson NMF. Here, \mathbf{x}_i denotes a row of \mathbf{X} and \mathbf{x}_j denotes a column of \mathbf{X} .

block-coordinate descent algorithm [64, 65], where the two “blocks” are \mathbf{H} and \mathbf{W} . It is analogous to “alternating least squares” for matrix factorization with Gaussian errors.

We point out two simple but important facts. First, by symmetry of (21), optimizing \mathbf{H} given \mathbf{W} has the same form as optimizing \mathbf{W} given \mathbf{H} . Second, because of the separability of the sum in (21), optimizing \mathbf{W} given \mathbf{H} splits into m independent K -dimensional subproblems of the following form:

$$\begin{aligned} & \text{minimize } \ell_j(\mathbf{w}_j) := \sum_{i=1}^n \mathbf{h}_i^T \mathbf{w}_j - x_{ij} \log(\mathbf{h}_i^T \mathbf{w}_j) \\ & \text{subject to } \mathbf{w}_j \geq \mathbf{0}, \end{aligned} \quad (22)$$

for $j = 1, \dots, m$. (And similarly for optimizing \mathbf{H} given \mathbf{W} .) Because the m subproblems (22) are independent, their solutions can be pursued in parallel. While both of these observations are simple, *neither of them hold for the multinomial topic model due to the sum-to-one constraints.*

Subproblem (22) is itself a well-studied maximum-likelihood estimation problem [66–72]; it is equivalent to computing an MLE of $\mathbf{b} := (b_1, \dots, b_K)^T \geq \mathbf{0}$ in an additive Poisson regression model:

$$\begin{aligned} y_i & \sim \text{Poisson}(\mu_i), \\ \mu_i & = \sum_{k=1}^K a_{ik} b_k, \end{aligned} \quad (23)$$

in which $\mathbf{y} = (y_1, \dots, y_n)^T \in \mathbf{R}_+^n$ and $\mathbf{A} \in \mathbf{R}_+^{n \times K}$. Consider a function that returns an MLE of \mathbf{b} in (23),

$$\text{FIT-POIS-REG}(\mathbf{A}, \mathbf{y}) := \underset{\mathbf{b} \in \mathbf{R}_+^K}{\operatorname{argmax}} p_{\text{PR}}(\mathbf{y} \mid \mathbf{A}, \mathbf{b}), \quad (24)$$

where $p_{\text{PR}}(\mathbf{y} \mid \mathbf{A}, \mathbf{b})$ denotes the likelihood under the Poisson regression model. Any algorithm that solves (24) can be applied iteratively to solve the Poisson NMF problem (21). This idea, which we call “alternating Poisson regression for Poisson NMF”, is formalized in

Table 1: Relationship between maximum-likelihood estimation algorithms for the additive Poisson regression model, Poisson NMF, and the multinomial topic model. Abbreviations used: EM = expectation maximization, MU = multiplicative updates, CD = co-ordinate descent, CCD = cyclic co-ordinate descent, SCD = sequential co-ordinate descent.

additive Poisson regression	Poisson NMF	topic model
EM [71]	MU [3, 4]	EM [1]
CD [74]	CCD [47], SCD [48]	none

Algorithm 1. (Similarly, Frobenius-norm NMF is often solved by iteratively solving a series of non-negative least squares problems [52, 73].)

3.2 Specific Algorithms

We now consider different approaches to solving FIT-POIS-REG(\mathbf{A}, \mathbf{y}), which, when inserted into Algorithm 1, produce different Poisson NMF algorithms. These algorithms are closely connected to existing algorithms for Poisson NMF and/or the multinomial topic model (Table 1).

3.2.1 Expectation Maximization

There is a long history of solving the Poisson regression problem (24) by EM [66–72, 75–79]. The EM updates for this problem consist of iterating the following updates:

$$\bar{z}_{ik} = y_i a_{ik} b_k / \mu_i \quad (25)$$

$$b_k = \frac{\sum_{i=1}^n \bar{z}_{ik}}{\sum_{i=1}^n a_{ik}}, \quad (26)$$

where \bar{z}_{ik} represents a posterior expectation in an equivalent augmented model; see Appendix A.

This EM algorithm is closely connected to the multiplicative update rules for Poisson NMF [4]: combining the E step (25) and M step (26) with the substitutions used in Algorithm 1 yields

$$h_{ik}^{\text{new}} \leftarrow h_{ik} \times \frac{\sum_{j=1}^m x_{ij} w_{jk} / \lambda_{ij}}{\sum_{j=1}^m w_{jk}} \quad (27)$$

$$w_{jk}^{\text{new}} \leftarrow w_{jk} \times \frac{\sum_{i=1}^n x_{ij} h_{ik} / \lambda_{ij}}{\sum_{i=1}^n h_{ik}}, \quad (28)$$

which are precisely the multiplicative updates for Poisson NMF. See Appendix A for the derivation. Additionally, applying the PNMF-TO-MTM reparameterization to the multiplicative updates (27–28) recovers the EM updates for the multinomial topic model [9, 14, 33, 55]. See Appendix A for the derivation. Therefore, when FIT-POIS-REG(\mathbf{A}, \mathbf{y}) is solved using EM, Algorithm 1 can be viewed as implementing “stepwise” variants of the

multiplicative updates for Poisson NMF or EM for the multinomial topic model (Table 1). By “stepwise”, we mean that the update order suggested by Algorithm 1 is to iterate the E and M steps for the first row of \mathbf{H} , then for the second row of \mathbf{H} , and so on, followed by updates to rows of \mathbf{W} . This is in contrast to a typical EM algorithm in which all E-step updates are performed first, then all M-step updates are performed.

3.2.2 Co-ordinate Descent

Co-ordinate descent is an alternative to EM that iteratively optimizes a single co-ordinate b_k while the remaining co-ordinates are fixed (see also [74]). For the Poisson regression problem, each 1-d optimization is straightforward to implement via Newton’s method,

$$b_k^{\text{new}} \leftarrow \max\{0, b_k - \alpha_k g_k / q_k\}, \quad (29)$$

where $\alpha_k \geq 0$ is a step size that can be determined by a line search or some other method, and g_k and q_k are the partial derivatives with respect to the negative log-likelihood $\ell_{\text{PR}}(\mathbf{b}) := -\log p_{\text{PR}}(\mathbf{y} \mid \mathbf{A}, \mathbf{b})$,

$$g_k := \frac{\partial \ell_{\text{PR}}}{\partial b_k} = \sum_{i=1}^n a_{ik} \left(1 - \frac{y_i}{\mu_i}\right) \quad (30)$$

$$q_k := \frac{\partial^2 \ell_{\text{PR}}}{\partial b_k^2} = \sum_{i=1}^n \frac{y_i a_{ik}^2}{\mu_i^2}. \quad (31)$$

Several Poisson NMF algorithms, including cyclic co-ordinate descent (CCD) [47], sequential co-ordinate descent (SCD) [48] and scalar Newton (SN) [8], can be viewed as implementing variants of this CD approach. That is, these approaches are essentially Algorithm 1 in which FIT-POIS-REG(\mathbf{A}, \mathbf{y}) is solved by CD. The CCD and SCD methods appear to be independent developments of the same or very similar algorithm; they both take a full (feasible) Newton step, setting $\alpha_k = 1$ when $b_k - \alpha_k g_k / q_k > 0$. By foregoing a line search to determine α_k , the update is not guaranteed to decrease the objective $\ell_{\text{PR}}(\mathbf{b})$ [80]. The SN method was developed to remedy this, with a step size scheme that always produces a decrease (while avoiding the expense of a line search). However, [8] compared SN with CCD and they found that CCD usually performed best in real data sets despite not having a line search.

Although the CD approach is straightforward for Poisson NMF, it is not straightforward for the multinomial topic model due to the sum-to-one constraints. This probably explains why the CD approach has not been implemented for the multinomial topic model (Table 1).

4 Numerical Experiments

To summarize, we have described two variants of Algorithm 1 for Poisson NMF (Table 1): the first fits an “additive Poisson regression” model using EM, and is essentially the same as existing EM algorithms for Poisson NMF and the multinomial topic model (which includes the Poisson NMF multiplicative updates); the second uses co-ordinate descent (CD) to fit

the additive Poisson regression model, and has no equivalent among existing algorithms for the multinomial topic model. In the remainder, we refer to these two variants of Algorithm 1 as “EM” and “CD”.

We begin with an in-depth example on a real data set to illustrate the differences between the EM and CD algorithms. The data for this example are RNA-sequencing read counts for $n = 41$ samples and $m = 16,773$ genes from [81]. This data set provides a “ground truth” of sorts for fitting the topic model: the data are gene expression measurements taken after human MCF-7 cells were exposed to either ethanol (EtOH), retinoic acid (RA), TGF- β , or the combination of RA and TGF- β . Therefore, the topic model with $K = 3$ topics should reflect the three different exposures, and samples in the combined exposure should be modeled as a combination of the RA and TGF- β topics. Indeed, the MLE we obtained (by running the Poisson NMF algorithm for a long time, with CD updates) largely produced the expected result: the samples in the ethanol condition were mostly represented by a single topic (the “ethanol topic”); the samples in the combination treatment were roughly an even combination of the RA and TGF- β topics; and the samples exposed to either RA and TGF- β were represented as combinations of the ethanol and RA topics or the ethanol and TGF- β topics (Figure 1A). The steps taken to prepare these data for topic modeling are detailed in Appendix C. The code implementing this experiment is provided in a Zenodo repository [82], and is available online at <https://github.com/stephenslab/fastTopics-experiments/>.

To compare the performance of the EM and CD variants on this data set, we first initialized the Poisson NMF parameters at random, then we ran 4 EM updates to slightly improve upon this random initialization. The resulting initial estimate of \mathbf{L} is shown in Figure 1A. Next, starting from this initial estimate, we ran 200 EM updates or 200 CD updates. (By “update”, we mean one iteration of the outer loop of Algorithm 1.) The CD updates produced estimates very close to the MLE; the distance to the MLE in log-likelihood units was just 0.079 (Figure 1B). By contrast, the EM estimates remained very far away from the MLE after 200 iterations, at a distance of over 150,000 log-likelihood units (Figure 1B). The EM estimates after 200 iterations were also *qualitatively* very different from the MLE (Figure 1A). These estimates are arguably less interpretable biologically since the topics do not map onto the treatments one-to-one.

To rule out the possibility the EM was just very unlucky and had settled into a different local maximum of the likelihood, we ran many more EM updates. Eventually, the EM updates recovered the same MLE (Figure 1C). Therefore, the very slow progress of EM could not be explained by having converged to a less optimal stationary point. One could conclude from this comparison that good estimates could be obtained simply by running the EM updates for a long time. However, this is often not practical for larger data sets.

Another algorithmic innovation we present here is the use of the extrapolation method [84] in accelerate convergence of the Poisson NMF algorithm. The idea behind the extrapolation method, which builds on the method of parallel tangents [85], is to avoid the “zigzagging” behaviour of the block-coordinate updates by iteratively adapting the step size according to the performance of the extrapolated updates compared to the non-extrapolated updates. The additional operations needed to implement the extrapolated updates impose minimal

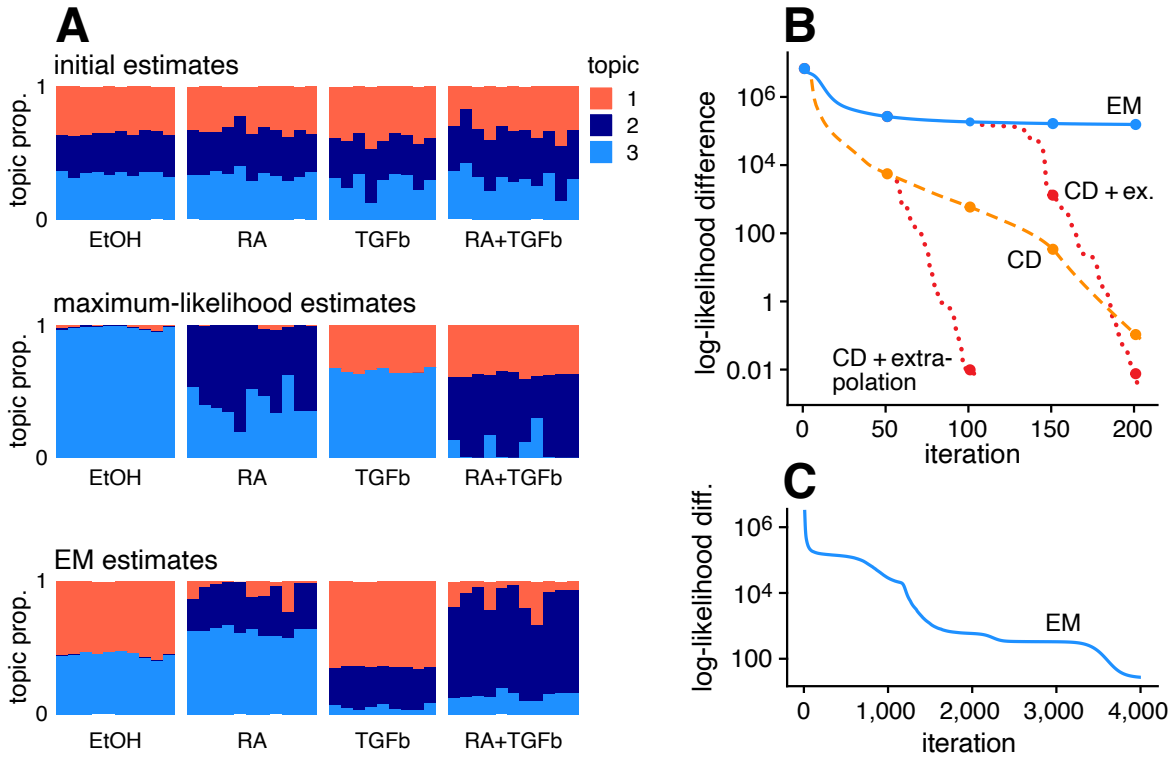


Figure 1: Results of fitting multinomial topic models to the MCF-7 data set [81], with $K = 3$ topics. Part A shows three estimates of the 41×3 matrix \mathbf{L} : the initial estimates (obtained by running a few EM updates); the MLE (obtained by running many CD updates, starting from the initial estimates); and the estimates obtained by running 200 EM updates starting from the initial estimates. Each estimate of the \mathbf{L} matrix is visualized using a “Structure plot” [83], which is a stacked bar chart in which the bar heights are given by the elements of \mathbf{L} . Part B shows the improvement in the multinomial topic model fits over time. Log-likelihoods are shown relative to the log-likelihood of the multinomial topic model at the MLE (A, middle row); points highest on the y-axis indicate the worst log-likelihoods.

overhead. The extrapolation method was originally applied to Frobenius-norm NMF, and to our knowledge it has not been used to accelerate algorithms for Poisson NMF, or for fitting topic models. (More details on the method and its implementation are given in [84] and in Appendix B.) To illustrate the benefits of extrapolation, we turned on the extrapolation at iteration 50 of the CD algorithm. Doing so allowed the CD updates to recover the MLE much more quickly than the non-extrapolated CD updates (Figure 1B). Furthermore, when we applied the extrapolated CD updates to the EM estimates, they were able to quickly “rescue” these poor-quality estimates (Figure 1B), illustrating that the slow progress of EM in this example was not due to some fundamental difficulty of the objective, but rather due to properties of the EM itself.

In summary, the results from this example suggest the potential for NMF methods—in particular, Algorithm 1 with CD updates plus extrapolation—to improve maximum-likelihood estimation for the multinomial topic model. To assess this more systematically, we performed comparisons of the EM and CD variants in a variety of data sets (Table 2):

Table 2: Data sets used in the experiments.

name	rows	columns	nonzeros
NeurIPS	2,483	14,036	3.7%
newsgroups	18,774	55,911	0.2%
epithelial airway	7,193	18,388	9.3%
68k PBMC	68,579	20,387	2.7%

two text data sets [86, 87] that have been used to evaluate topic modeling methods (e.g., [33, 88]); and two single-cell RNA sequencing (scRNA-seq) data sets [89, 90]. Appendix C gives additional details on these data sets and the experiment setup. All the algorithms compared in these experiments were implemented in the fastTopics R package (see the supplementary ZIP file). This R implementation includes the enhancements described in Appendix B intended to make the algorithms more efficient and numerically stable. The code implementing these experiments is provided in a Zenodo repository [82], and is available online at <https://github.com/stephenslab/fastTopics-experiments/>.

To reduce the possibility that multiple optimizations converge to different local maxima of the likelihood, which could complicate the comparisons, we first ran 1,000 EM updates—that is, 1,000 iterations of the outer loop of Algorithm 1—then we examined the performance of the algorithms *after* this initialization phase. Therefore, in our comparisons we assessed the extent to which the different algorithms improved upon this initialization. Another practical issue was that it was not always practical to run the optimization algorithms long enough to obtain an accurate MLE. Therefore, instead of comparing the estimates to the MLE, like we did in the example above, we used as a reference point the best estimate (in log-likelihood) that was obtained.

Selected results of these comparisons are shown in Figure 2, and more comprehensive results on all four data sets, with K ranging from 2 to 12, are given in the Appendix (Figures 5–12). In almost all cases, the extrapolated CD updates converged to an MLE at least as fast as the other algorithms, and often much faster, or produced the best fit within the allotted time. The extrapolation method generally helped convergence of CD, and sometimes helped EM. Also, the per-iteration running time per was very similar in all the algorithms. Beyond this, there was considerable variation in the algorithms’ performance among the different data sets and within each data set at different settings of K . To make sense of the diverse results, we distinguish three main patterns.

A1 and B1 in Figure 2 illustrate the first pattern: EM quickly progressed to a good solution, and so any improvements over EM were small regardless of the algorithm used. Indeed, despite the small improvements in log-likelihood obtained by the CD estimates in A1 and B1, the final EM and CD estimates were nearly indistinguishable from each other (Figure 2, A2 and B2).

C1 and D1 in Figure 2 illustrate the second pattern: the initial 1,000 iterations of EM was

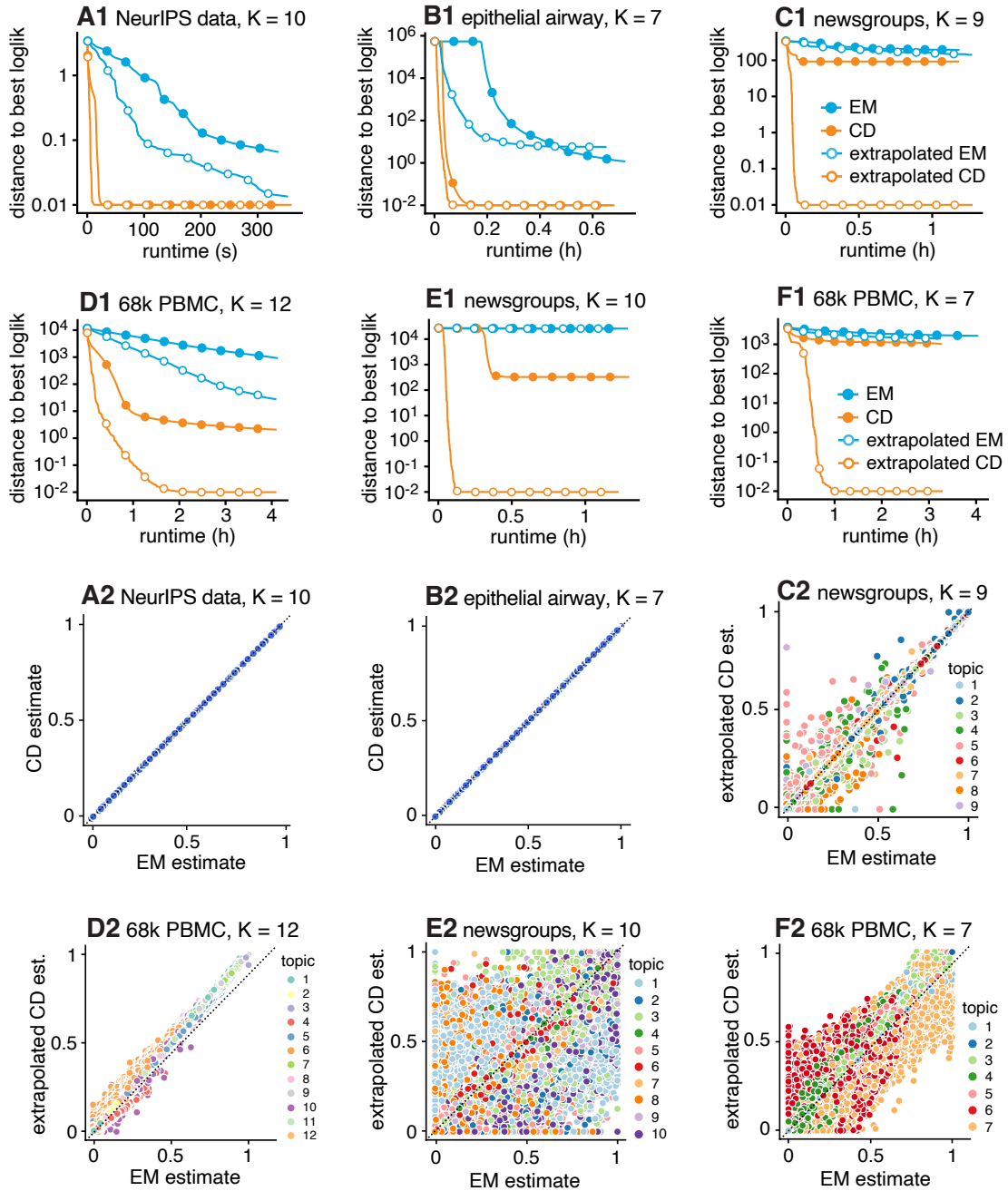


Figure 2: Selected results on fitting topic models using Poisson NMF algorithms. In A1–F1, multinomial log-likelihoods are given relative to the best log-likelihood obtained among the four algorithms compared (EM and CD, with and without extrapolation). Log-likelihood differences less than 0.01 are shown as 0.01, and circles are drawn at intervals of 100 iterations. The 1,000 EM iterations performed during the initialization phase are not shown. Plots A2–F2 compare the final estimates of \mathbf{L} from in A1–F1. See also Figures 5–12 in the Appendix for additional results obtained with different settings of K .

insufficient to recover estimates close to an MLE, and running additional updates sometimes substantially improved the fit. Among the four algorithms compared, the extrapolated CD

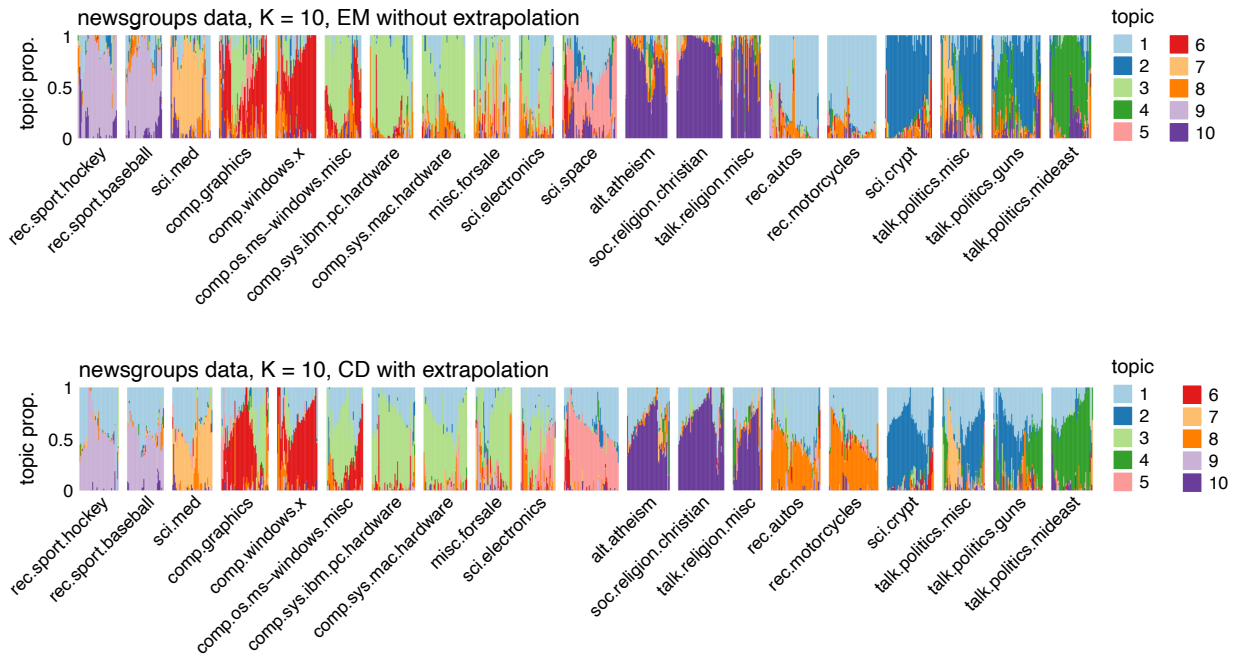


Figure 3: Estimates of \mathbf{L} from the newsgroups data, with $K = 10$ topics, obtained by running the EM updates without extrapolation and the CD updates with extrapolation. The estimates of \mathbf{L} are visualized using Structure plots. The documents are arranged by newsgroup to show the correspondence between the newsgroups and the topics. Note that the ordering of the documents within each newsgroup is not exactly the same in the top and bottom Structure plots. See E1 and E2 in Figure 2 for related results.

updates again provided the greatest improvement in log-likelihood within the allotted time. And yet, despite the considerable improvements in log-likelihood, the final estimates did not change much (Figure 2, C2 and D2). So while the CD updates can sometimes produce large gains in computational performance, these gains do not always have a meaningful impact on the topic modeling results.

E1 and F1 in Figure 2 are examples of the third pattern: the extrapolated CD updates not only produced estimates with greatly improved log-likelihood, they also produced estimates that were *qualitatively very different* (Figure 2, E2 and F2). In both this and the previous pattern, the EM updates progressed slowly toward a solution. But whereas this slow progress was benign in the previous examples, with little impact on the final result (and perhaps could even be beneficial by implicitly regularizing the estimates), in these examples the slow progress of EM was in an area of the likelihood that was very far away from an MLE. We also observed an example of this pattern earlier in the MCF-7 data set (Figure 1). In brief, the slow convergence of the EM updates is sometimes benign, and sometimes not, but it is impossible to know in advance which it is without making these comparisons. Therefore, one way to avoid this problem is to use the CD updates, which are generally better at not getting stuck in areas of the likelihood far away from an MLE.

We also examined the topic model estimates in E and F to understand how the improved estimates can affect our understanding of the data. In the newsgroups data (Figure 3), topics

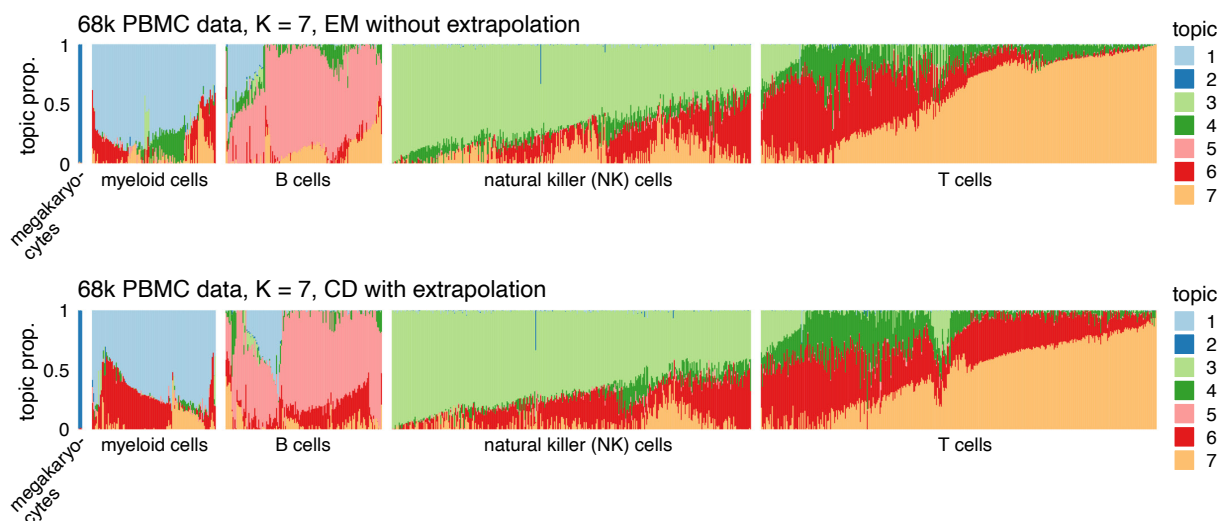


Figure 4: Estimates of \mathbf{L} from the 68k PBMC data, with $K = 7$ topics, obtained by running the EM updates without extrapolation and the CD updates with extrapolation. The estimates of \mathbf{L} are visualized using Structure plots. To facilitate comparison, the cells were split into 5 groups based on the CD estimates of \mathbf{L} ; these groups roughly correspond to cell types (B cells, T cells, etc). The “T cells” group was downsampled to better visualize the other groups. Note that the ordering of the cells within each grouping is exactly not the same in the top and bottom Structure plots. See F1 and F2 in Figure 2 for related results.

1 and 8 changed most between the EM and CD estimates: in the EM estimates, the rec.auto and rec.motorcycle newsgroup discussions were largely captured by topic 1 which was also shared by most other newsgroups (a “background topic”); in the CD estimates, topic 8 better distinguished rec.auto and rec.motorcycle from the other newsgroups, and topic 1, the “background topic”, was (appropriately) present more evenly in all the newsgroups.

In the 68k PBMC data (Figure 4), there were many differences between the EM and CD estimates, but the changes to topic 4 most affect our understanding of these data: in the EM estimates, the T cells shared topic 4 with a subset of myeloid cells—suggesting some sort of pathway or gene expression program common to myeloid and T cells—but in the improved CD estimates, this connection between myeloid and T cells largely disappeared, and topic 4 was nearly unique to T cells.

5 Discussion

In this paper, we suggested a simple strategy for fitting topic models by exploiting the equivalence of Poisson NMF and the multinomial topic model: first fit a Poisson NMF, then recover the corresponding topic model. To our knowledge, this equivalence, despite being informally recognized early on in the development of these methods, has not been previously exploited to fit topic models. The greatest improvements in optimization performance were achieved when the Poisson NMF was optimized using a simple co-ordinate descent (CD) algorithm. While the CD algorithm may be simple, consider that, due to the “sum-to-one”

constraints, it is not obvious how to implement CD for the multinomial topic model.

For many statistical applications, point estimation such as maximum-likelihood estimation will suffice when the main aim is to learn a low-rank representation of the count data (see also [53] for other arguments supporting point estimation in topic models). Further, focussing on point estimation simplifies numerical computation, allowing for simpler and efficient algorithms that can be quickly applied to large data sets. We focussed on maximum-likelihood estimation, but the ideas and algorithms presented here also apply to MAP estimation with Dirichlet priors on \mathbf{F} . Extending these ideas to improve variational inference algorithms for topic models (e.g., LDA) may also be of interest. Given the success of the CD approach, it may be fruitful to develop CD-based variational inference algorithms for LDA and Poisson NMF [91]. That said, in many applications topic models are mainly used for dimension reduction—the goal being to learn compact representations of complex patterns—and in these applications, maximum-likelihood or MAP estimation may suffice. Some topic modeling applications involve massive data sets that require an “online” approach [34, 35, 92, 93]. Developing online versions of our algorithms is straightforward in principle, although online learning brings additional practical challenges, such as the choice of learning rates.

It is well known that EM can suffer from slow convergence; recent theoretical developments [39, 40] shed some light on this slow convergence and the conditions under which it occurs. And so it is perhaps not surprising that the EM variant of the Alternating Poisson Regression algorithm (Algorithm 1) was also very slow in some data sets. However, we distinguished between two types of slow convergence: benign slow convergence that occurs when the EM estimates are near an MLE; and slow convergence far away from an MLE, which can result in EM estimates that are very different from an MLE, and can affect how the topics are interpreted. Several methods have been developed specifically to accelerate EM [41–43], and therefore it would have been natural to apply these methods here to improve the performance of the EM updates. We actually tried two more recent acceleration methods—DAAREM [43] and the quasi-Newton method of [41]—but in our tests (results not shown) we found that both methods provided little improvement over the unaccelerated EM. (Taddy [53] also used quasi-Newton to accelerate EM, but did not provide any results to show that this was beneficial.) The only acceleration method that consistently improved performance was the extrapolation method of [84] specifically developed for NMF.

Acknowledgements

Many people have contributed helpful ideas and feedback, including Mihai Anitescu, Kushal Dey, Adam Gruenbaum, Joyce Hsiao, Anthony Hung, Youngseok Kim, Kaixuan Luo, John Novembre, Sebastian Pott, Alan Selewa, Eric Weine and Jason Willwerscheid. We thank Xihui Lin, Paul Boutros, Minzhe Wang and Tracy Ke for helpful R code. And we thank the staff at the Research Computing Center for providing the high-performance computing resources used to implement the numerical experiments.

Disclosure Statement

No conflicts of interest were reported by the authors.

Data Availability Statement

All the data sets used in this paper are openly available: the NeurIPS data set was obtained from <http://ai.stanford.edu/~gal/data.html>; the newsgroups data set was downloaded from <http://qwone.com/~jason/20Newsgroups>; the MCF-7 and epithelial airway data sets were downloaded from the Gene Expression Omnibus (GEO) website, accessions GSE152749 and GSE103354; and the 68k PBMC data set was downloaded from the 10x Genomics website, <https://www.10xgenomics.com/datasets>.

Funding

This work was supported by the NHGRI at the National Institutes of Health under award number R01HG002585.

SUPPLEMENTARY MATERIAL

fastTopics 0.7-25: The fastTopics R package providing efficient implementations of the methods described in this paper. (ZIP file)

References

- [1] T. Hofmann. Probabilistic latent semantic indexing. In *Proceedings of the 22nd Annual International ACM SIGIR Conference*, pages 50–57, 1999.
- [2] S. Arora, R. Ge, and A. Moitra. Learning topic models—going beyond SVD. In *53rd IEEE Annual Symposium on Foundations of Computer Science*, 2012.
- [3] D. D. Lee and H. S. Seung. Learning the parts of objects by non-negative matrix factorization. *Nature*, 401(6755):788–791, 1999.
- [4] D. D. Lee and H. S. Seung. Algorithms for non-negative matrix factorization. In *Advances in Neural Information Processing Systems*, volume 13, pages 556–562, 2001.
- [5] A. Cichocki, S. Cruces, and S.-I. Amari. Generalized alpha-beta divergences and their application to robust nonnegative matrix factorization. *Entropy*, 13(1):134–170, 2011.
- [6] I. S. Dhillon and S. Sra. Generalized nonnegative matrix approximations with Bregman divergences. In *Advances in Neural Information Processing Systems*, volume 18, pages 283–290, 2005.
- [7] C. Févotte and J. Idier. Algorithms for nonnegative matrix factorization with the β -divergence. *Neural Computation*, 23(9):2421–2456, 2011.
- [8] L. T. K. Hien and N. Gillis. Algorithms for nonnegative matrix factorization with the Kullback–Leibler divergence. *Journal of Scientific Computing*, 87(3):93, 2021.
- [9] W. Buntine. Variational extensions to EM and multinomial PCA. In *Proceedings of the 13th European Conference on Machine Learning*, pages 23–34, 2002.

- [10] W. Buntine and A. Jakulin. Discrete component analysis. In M. Saunders, Craigand Grobelnik, S. Gunn, and J. Shawe-Taylor, editors, *Subspace, latent structure and feature selection*, volume 3940 of *Lecture Notes in Computer Science*, 2006.
- [11] J. Canny. GaP: a factor model for discrete data. In *Proceedings of the 27th Annual International ACM SIGIR Conference*, pages 122–129, 2004.
- [12] C. Ding, T. Li, and W. Peng. On the equivalence between non-negative matrix factorization and probabilistic latent semantic indexing. *Computational Statistics and Data Analysis*, 52(8):3913–3927, 2008.
- [13] T. Faleiros and A. Lopes. On the equivalence between algorithms for non-negative matrix factorization and latent Dirichlet allocation. In *Proceedings of the 24th European Symposium on Artificial Neural Networks*, pages 171–176, 2016.
- [14] E. Gaussier and C. Goutte. Relation between PLSA and NMF and implications. In *Proceedings of the 28th Annual International ACM SIGIR Conference*, pages 601–602, 2005.
- [15] N. Gillis. *Nonnegative matrix factorization*. Society for Industrial and Applied Mathematics, Philadelphia, PA, 2021.
- [16] M. Zhou, L. Hannah, D. Dunson, and L. Carin. Beta-negative binomial process and Poisson factor analysis. In *Proceedings of the 15th International Conference on Artificial Intelligence and Statistics*, pages 1462–1471, 2012.
- [17] M. Chirichella, M. Ratcliff, S. Gu, R. Miragaia, M. Sammito, V. Cutano, S. Cohen, D. Angeletti, X. Romero-Ros, and D. J. Schofield. Integrated single-cell analyses of affinity-tested b-cells enable the identification of a gene signature to predict antibody affinity. *bioRxiv*, doi:10.1101/2025.01.15.633143, 2025.
- [18] P. Carbonetto, K. Luo, A. Sarkar, A. Hung, K. Tayeb, S. Pott, and M. Stephens. GoM DE: interpreting structure in sequence count data with differential expression analysis allowing for grades of membership. *Genome Biology*, 24:236, 2023.
- [19] B. D. Umans and Y. Gilad. Oxygen-induced stress reveals context-specific gene regulatory effects in human brain organoids. *Genome Research*, doi:10.1101/gr.280219.124, 2025.
- [20] R. Meir, G. Schwartz, M. Adam, A. A. Lapidot, A. Cain, G. S. Green, V. Menon, D. A. Bennett, P. L. De Jager, and N. Habib. Early neuronal reprogramming and cell cycle reentry shape Alzheimer’s disease progression. *bioRxiv*, doi:10.1101/2025.06.04.653670, 2025.
- [21] C. F. Gao, S. Vaikuntanathan, and S. J. Riesenfeld. Dissection and integration of bursty transcriptional dynamics for complex systems. *Proceedings of the National Academy of Sciences*, 121(18):e2306901121, 2024.
- [22] J. M. Popp, K. Rhodes, R. Jangi, M. Li, K. Barr, K. Tayeb, A. Battle, and Y. Gilad. Cell type and dynamic state govern genetic regulation of gene expression in heterogeneous differentiating cultures. *Cell Genomics*, 4(12):100701, 2024.
- [23] Z. Liang, H. D. Anderson, V. Locher, C. O’Leary, S. J. Riesenfeld, B. Jabri, B. D.

- McDonald, and A. Bendelac. Eomes expression identifies the early bone marrow precursor to classical NK cells. *Nature Immunology*, 25(7):1172–1182, 2024.
- [24] Y. Zhao, R. Zhou, Z. Mu, P. Carbonetto, X. Zhong, B. Xie, K. Luo, C. M. Cham, J. Koval, X. He, A. W. Dahl, X. Liu, E. B. Chang, A. Basu, and S. Pott. Cell-type-resolved chromatin accessibility in the human intestine identifies complex regulatory programs and clarifies genetic associations in Crohn’s disease. *medRxiv*, doi:10.1101/2024.12.10.24318718, 2024.
- [25] G. Housman, E. Briscoe, and Y. Gilad. Evolutionary insights into primate skeletal gene regulation using a comparative cell culture model. *PLoS Genetics*, 18(3):e1010073, 2022.
- [26] A. Hung, G. Housman, E. Briscoe, C. Cuevas, and Y. Gilad. Characterizing gene expression in an in vitro biomechanical strain model of joint health [version 2; peer review: 1 approved, 1 not approved]. *F1000Research*, 11:296, 2022.
- [27] K. Rhodes, K. A. Barr, J. M. Popp, B. J. Strober, A. Battle, and Y. Gilad. Human embryoid bodies as a novel system for genomic studies of functionally diverse cell types. *eLife*, 11:e71361, 2022.
- [28] S. Bastide, E. Chomsky, B. Saudemont, Y. Loe-Mie, S. Schmutz, S. Novault, H. Marlow, A. Tanay, and F. Spitz. TATTOO-seq delineates spatial and cell type-specific regulatory programs in the developing limb. *Science Advances*, 8(50):eadd0695, 2022.
- [29] K. K. Dey, C. J. Hsiao, and M. Stephens. Visualizing the structure of RNA-seq expression data using grade of membership models. *PLoS Genetics*, 13(3):e1006599, 2017.
- [30] C. González-Blas, L. Minnoye, D. Papasokrati, S. Aibar, G. Hulselmans, V. Christiaens, K. Davie, J. Wouters, and S. Aerts. cisTopic: cis-regulatory topic modeling on single-cell ATAC-seq data. *Nature Methods*, 16(5):397–400, 2019.
- [31] D. M. Blei, A. Y. Ng, and M. I. Jordan. Latent Dirichlet allocation. *Journal of Machine Learning Research*, 3:993–1022, 2003.
- [32] Y. W. Teh, D. Newman, and M. Welling. A collapsed variational Bayesian inference algorithm for latent Dirichlet allocation. In *Advances in Neural Information Processing Systems*, volume 19, pages 1353–1360, 2007.
- [33] A. Asuncion, M. Welling, P. Smyth, and Y. W. Teh. On smoothing and inference for topic models. In *Proceedings of the 25th Conference on Uncertainty in Artificial Intelligence*, pages 27–34, 2009.
- [34] M. Hoffman, F. Bach, and D. Blei. Online learning for latent Dirichlet allocation. In *Advances in Neural Information Processing Systems*, volume 23, pages 856–864, 2010.
- [35] M.-A. Sato. Online model selection based on the variational Bayes. *Neural Computation*, 13(7):1649–1681, 2001.
- [36] T. L. Griffiths and M. Steyvers. Finding scientific topics. *Proceedings of the National Academy of Sciences*, 101(Supplement 1):5228–5235, 2004.
- [37] R. A. Redner and H. F. Walker. Mixture densities, maximum likelihood and the EM

- algorithm. *SIAM Review*, 26(2):195–239, 1984.
- [38] J. Ma, L. Xu, and M. I. Jordan. Asymptotic convergence rate of the EM algorithm for Gaussian mixtures. *Neural Computation*, 12(12):2881–2907, 2000.
 - [39] R. Dwivedi, N. Ho, K. Khamaru, M. J. Wainwright, M. I. Jordan, and B. Yu. Singularity, misspecification and the convergence rate of EM. *Annals of Statistics*, 48(6), 2020.
 - [40] F. Kunstner, R. Kumar, and M. Schmidt. Homeomorphic-invariance of EM: Non-asymptotic convergence in KL divergence for exponential families via mirror descent. In A. Banerjee and K. Fukumizu, editors, *Proceedings of the 24th International Conference on Artificial Intelligence and Statistics*, pages 3295–3303, 2021.
 - [41] H. Zhou, D. Alexander, and K. Lange. A quasi-Newton acceleration for high-dimensional optimization algorithms. *Statistics and Computing*, 21(2):261–273, 2011.
 - [42] R. Varadhan and C. Roland. Simple and globally convergent methods for accelerating the convergence of any EM algorithm. *Scandinavian Journal of Statistics*, 35(2):335–353, 2008.
 - [43] N. C. Henderson and R. Varadhan. Damped Anderson acceleration with restarts and monotonicity control for accelerating EM and EM-like algorithms. *Journal of Computational and Graphical Statistics*, 28(4):834–846, 2019.
 - [44] A. Ali, J. Z. Kolter, and R. J. Tibshirani. A continuous-time view of early stopping for least squares regression. In K. Chaudhuri and M. Sugiyama, editors, *Proceedings of the 22nd International Conference on Artificial Intelligence and Statistics*, pages 1370–1378, 2019.
 - [45] S. Gunasekar, B. E. Woodworth, S. Bhojanapalli, B. Neyshabur, and N. Srebro. Implicit regularization in matrix factorization. In I. Guyon, U. V. Luxburg, S. Bengio, H. Wallach, R. Fergus, S. Vishwanathan, and R. Garnett, editors, *Advances in Neural Information Processing Systems*, volume 30, 2017.
 - [46] A. T. Cemgil. Bayesian inference for nonnegative matrix factorisation models. *Computational Intelligence and Neuroscience*, 2009:785152, 2009.
 - [47] C.-J. Hsieh and I. S. Dhillon. Fast coordinate descent methods with variable selection for non-negative matrix factorization. In *Proceedings of the 17th ACM SIGKDD International Conference*, pages 1064–1072, 2011.
 - [48] X. Lin and P. C. Boutros. Optimization and expansion of non-negative matrix factorization. *BMC Bioinformatics*, 21:7, 2020.
 - [49] S. Arora, R. Ge, Y. Halpern, D. Mimno, A. Moitra, D. Sontag, Y. Wu, and M. Zhu. A practical algorithm for topic modeling with provable guarantees. In *Proceedings of the 30th International Conference on Machine Learning*, pages 280–288, 2013.
 - [50] D. Donoho and V. Stodden. When does non-negative matrix factorization give a correct decomposition into parts? In *Advances in Neural Information Processing Systems*, volume 16, 2003.
 - [51] N. Gillis and S. A. Vavasis. Semidefinite programming based preconditioning for more robust near-separable nonnegative matrix factorization. *SIAM Journal on Optimization*,

- 25(1):677–698, 2015.
- [52] J. Kim, Y. He, and H. Park. Algorithms for nonnegative matrix and tensor factorizations: a unified view based on block coordinate descent framework. *Journal of Global Optimization*, 58(2):285–319, 2014.
 - [53] M. Taddy. On estimation and selection for topic models. In *Proceedings of the 15th International Conference on Artificial Intelligence and Statistics*, volume 22, pages 1184–1193, 2012.
 - [54] T. Hofmann, J. Puzicha, and M. Jordan. Learning from dyadic data. In *Advances in Neural Information Processing Systems*, volume 11, pages 466–472, 1999.
 - [55] T. Hofmann. Unsupervised learning by probabilistic latent semantic analysis. *Machine Learning*, 42(1):177–196, 2001.
 - [56] A. P. Singh and G. J. Gordon. A unified view of matrix factorization models. In *Joint European Conference on Machine Learning and Knowledge Discovery in Databases*, volume 2, pages 358–373, 2008.
 - [57] M. Steyvers and T. Griffiths. Probabilistic topic models. In T. Landauer, D. McNamara, S. Dennis, and W. Kintsch, editors, *Latent semantic analysis: a road to meaning*, pages 427–448. Lawrence Erlbaum Associates, Mahwah, NJ, 2007.
 - [58] R. A. Fisher. On the interpretation of χ^2 from contingency tables, and the calculation of P. *Journal of the Royal Statistical Society*, 85(1):87–94, 1922.
 - [59] I. J. Good. Some statistical applications of Poisson’s work. *Statistical Science*, 1(2):157–170, 1986.
 - [60] S. Boyd and L. Vandenberghe. *Convex optimization*. Cambridge University Press, New York, NY, 2004.
 - [61] D. Sontag and D. Roy. Complexity of inference in latent Dirichlet allocation. In *Advances in Neural Information Processing Systems*, volume 24, pages 1008–1016, 2011.
 - [62] H. Ma, C. Liu, I. King, and M. R. Lyu. Probabilistic factor models for web site recommendation. In *Proceedings of the 34th International ACM SIGIR Conference on Research and Development in Information Retrieval*, pages 265–274, 2011.
 - [63] S. A. Vavasis. On the complexity of nonnegative matrix factorization. *SIAM Journal on Optimization*, 20(3):1364–1377, 2010.
 - [64] S. J. Wright. Coordinate descent algorithms. *Mathematical Programming*, 151:3–34, 2015.
 - [65] D. P. Bertsekas. *Nonlinear programming*. Athena Scientific, Belmont, MA, 2nd edition, 1999.
 - [66] G. J. McLachlan and T. Krishnan. *The EM algorithm and extensions*. Wiley-Interscience, Hoboken, NJ, 2008.
 - [67] K. Lange and R. Carson. EM reconstruction algorithms for emission and transmission tomography. *Journal of Computer Assisted Tomography*, 8(2):306–316, 1984.
 - [68] L. Lucy. An iterative algorithm for the rectification of observed distributions. *The*

- Astronomical Journal*, 79:745–754, 1974.
- [69] R. Molina, J. Nunez, F. Cortijo, and J. Mateos. Image restoration in astronomy: a Bayesian perspective. *IEEE Signal Processing Magazine*, 18(2):11–29, 2001.
 - [70] W. H. Richardson. Bayesian-based iterative method of image restoration. *Journal of the Optical Society of America*, 62(1):55–59, 1972.
 - [71] L. A. Shepp and Y. Vardi. Maximum likelihood reconstruction for emission tomography. *IEEE Transactions on Medical Imaging*, 1(2):113–122, 1982.
 - [72] Y. Vardi, L. A. Shepp, and L. Kaufman. A statistical model for positron emission tomography. *Journal of the American Statistical Association*, 80(389):8–20, 1985.
 - [73] N. Gillis. The why and how of nonnegative matrix factorization. *arXiv*, 1401.5226, 2014.
 - [74] C. Bouman and K. Sauer. A unified approach to statistical tomography using coordinate descent optimization. *IEEE Transactions on Image Processing*, 5(3):480–492, 1996.
 - [75] A. P. Dempster, N. M. Laird, and D. B. Rubin. Maximum likelihood from incomplete data via the EM algorithm. *Journal of the Royal Statistical Society, Series B*, 39:1–22, 1977.
 - [76] A. De Pierro. On the relation between the ISRA and the EM algorithm for positron emission tomography. *IEEE Transactions on Medical Imaging*, 12(2):328–333, 1993.
 - [77] T. Krishnan. EM algorithm in tomography: a review and a bibliography. *Bulletin of Informatics and Cybernetics*, 27:5–22, 1995.
 - [78] X.-L. Meng and D. Van Dyk. The EM algorithm—an old folk-song sung to a fast new tune. *Journal of the Royal Statistical Society, Series B*, 59(3):511–567, 1997.
 - [79] Y. Vardi and D. Lee. From image deblurring to optimal investments: maximum likelihood solutions for positive linear inverse problems. *Journal of the Royal Statistical Society, Series B*, 55(3):569–598, 1993.
 - [80] J. Nocedal and S. J. Wright. *Numerical optimization*. Springer, New York, NY, 2nd edition, 2006.
 - [81] E. M. Sanford, B. L. Emert., A. Coté, and A. Raj. Gene regulation gravitates toward either addition or multiplication when combining the effects of two signals. *eLife*, 9: e59388.
 - [82] P. Carbonetto, A. Sarkar, Z. Wang, and M. Stephens. Code and data used to generate the results for this paper, 2024. doi:10.5281/zenodo.15793270.
 - [83] N. A. Rosenberg. Genetic structure of human populations. *Science*, 298(5602):2381–2385, 2002.
 - [84] A. M. S. Ang and N. Gillis. Accelerating nonnegative matrix factorization algorithms using extrapolation. *Neural Computation*, 31(2):417–439, 2019.
 - [85] D. G. Luenberger and Y. Ye. *Linear and nonlinear programming*. Springer, 4th edition, 2015.
 - [86] A. Globerson, G. Chechik, F. Pereira, and N. Tishby. Euclidean embedding of co-

- occurrence data. *Journal of Machine Learning Research*, 8:2265–2295, 2007.
- [87] J. Rennie. 20 newsgroups data set, 2007. <http://qwone.com/~jason/20Newsgroups>.
 - [88] H. M. Wallach. Topic modeling: beyond bag-of-words. In *Proceedings of the 23rd International Conference on Machine Learning*, pages 977–984, 2006.
 - [89] D. T. Montoro, A. L. Haber, M. Biton, V. Vinarsky, B. Lin, S. E. Birket, et al. A revised airway epithelial hierarchy includes CFTR-expressing ionocytes. *Nature*, 560(7718):319–324, 2018.
 - [90] G. X. Y. Zheng, J. M. Terry, P. Belgrader, P. Ryvkin, Z. W. Bent, R. Wilson, et al. Massively parallel digital transcriptional profiling of single cells. *Nature Communications*, 8:14049, 2017.
 - [91] P. Gopalan, J. M. Hofman, and D. M. Blei. Scalable recommendation with hierarchical Poisson factorization. In *Proceedings of the 31st Conference on Uncertainty in Artificial Intelligence*, pages 326–335, 2015.
 - [92] M. D. Hoffman, D. M. Blei, C. Wang, and J. Paisley. Stochastic variational inference. *Journal of Machine Learning Research*, 14(40):1303–1347, 2013.
 - [93] T. Broderick, N. Boyd, A. Wibisono, A. C. Wilson, and M. I. Jordan. Streaming variational Bayes. In C. Burges, L. Bottou, M. Welling, Z. Ghahramani, and K. Weinberger, editors, *Advances in Neural Information Processing Systems*, volume 26, 2013.
 - [94] N. Gillis and F. Glineur. Accelerated multiplicative updates and hierarchical ALS algorithms for nonnegative matrix factorization. *Neural Computation*, 24(4):1085–1105, 2012.
 - [95] G. Contreras and M. Martonosi. Characterizing and improving the performance of Intel Threading Building Blocks. In *IEEE International Symposium on Workload Characterization*, pages 57–66, 2008.
 - [96] R Core Team. *R: a language and environment for statistical computing*. R Foundation for Statistical Computing, Vienna, Austria, 2018. <https://www.R-project.org>.
 - [97] D. Eddelbuettel and R. François. Rcpp: seamless R and C++ integration. *Journal of Statistical Software*, 40(8):1–18, 2011.
 - [98] J. D. Blischak, P. Carbonetto, and M. Stephens. Creating and sharing reproducible research code the workflowr way [version 1; peer review: 3 approved]. *F1000Research*, 8(1749), 2019.

A Derivations and Additional Theory

A.1 MAP Estimation

Corollary 2 (Relationship between MAP estimates for Poisson NMF and the multinomial topic model). Let $\hat{\mathbf{H}} \in \mathbf{R}_+^{n \times K}$, $\hat{\mathbf{W}} \in \mathbf{R}_+^{m \times K}$ denote *maximum a posteriori* (MAP) estimates for the Poisson NMF model, in which elements of \mathbf{W} are assigned independent gamma priors, $w_{jk} \sim \text{Gamma}(a_{jk}, b_k)$, with $a_{jk} > 1$, $b_k > 0$, for $j = 1, \dots, m$, $k = 1, \dots, K$, and

elements of \mathbf{H} are assigned an (improper) uniform prior,

$$\hat{\mathbf{H}}, \hat{\mathbf{W}} \in \operatorname{argmax}_{\mathbf{H}, \mathbf{W}} p_{\text{PNMF}}(\mathbf{X} \mid \mathbf{H}, \mathbf{W}) p_{\text{gamma}}(\mathbf{W}), \quad (32)$$

in which

$$p_{\text{gamma}}(\mathbf{W}) := \prod_{j=1}^m \prod_{k=1}^K \text{Gamma}(w_{jk}; a_{jk}, b_k),$$

and where $\text{Gamma}(\theta; \alpha, \beta) \propto \theta^{\alpha-1} e^{-\beta\theta}$ denotes the probability density of the gamma distribution with shape α and rate (inverse scale) β . If $\hat{\mathbf{L}}, \hat{\mathbf{F}}$ are obtained by applying PNMF-TO-MTM to $\hat{\mathbf{H}}, \hat{\mathbf{W}}$, these are MAP estimates for the multinomial topic model with independent Dirichlet priors on the columns of \mathbf{F} , $f_{1k}, \dots, f_{mk} \sim \text{Dirichlet}(a_{1k}, \dots, a_{mk})$ and a uniform prior on \mathbf{L} ,

$$\hat{\mathbf{L}}, \hat{\mathbf{F}} \in \operatorname{argmax}_{\mathbf{L}, \mathbf{F}} p_{\text{MTM}}(\mathbf{X} \mid \mathbf{L}, \mathbf{F}) p_{\text{dirichlet}}(\mathbf{F}) \quad (33)$$

in which

$$p_{\text{dirichlet}}(\mathbf{F}) := \prod_{k=1}^K \text{Dirichlet}(f_{1k}, \dots, f_{mk}; a_{1k}, \dots, a_{mk}),$$

and where $\text{Dirichlet}(\theta_1, \dots, \theta_d; \alpha_1, \dots, \alpha_d) \propto \theta_1^{\alpha_1-1} \dots \theta_d^{\alpha_d-1}$ denotes the probability density of the Dirichlet distribution with parameters $\alpha_1, \dots, \alpha_d$. Conversely, let $\hat{\mathbf{L}} \in \mathbf{R}_{\text{row}}^{n \times K}$, $\hat{\mathbf{F}} \in \mathbf{R}_{\text{col}}^{m \times K}$ denote multinomial topic model MAP estimates (33), set $\hat{s}_i = t_i = \sum_{j=1}^m x_{ij}$, for $i = 1, \dots, n$, and set $\hat{u}_k = \sum_{j=1}^m (a_{jk} - 1)/b_k$, for $k = 1, \dots, K$. Then if $\hat{\mathbf{H}}, \hat{\mathbf{W}}$ are obtained by applying MTM-TO-PNMF to $\hat{\mathbf{L}}, \hat{\mathbf{F}}, \hat{\mathbf{s}}, \hat{\mathbf{u}}$, these will be Poisson NMF MAP estimates (32).

Proof. To prove this result, first note that minimizing the penalized objective for the multinomial topic model, $\phi^*(\mathbf{L}, \mathbf{F})$ (see eq. 17), corresponds to computing MAP estimates (33). This penalized objective can be written in the form of the unpenalized objective, $\phi(\mathbf{L}, \mathbf{F})$: $\operatorname{argmax}_{\mathbf{L}, \mathbf{F}} \phi^*(\mathbf{X}; \mathbf{L}, \mathbf{F}) = \operatorname{argmax}_{\mathbf{L}, \mathbf{F}} \phi(\tilde{\mathbf{X}}; \tilde{\mathbf{L}}, \mathbf{F})$, where $\tilde{\mathbf{X}}$ and $\tilde{\mathbf{L}}$ are matrices augmented with an additional K “pseudodocuments”:

$$\tilde{\mathbf{X}} := \begin{bmatrix} \mathbf{X} \\ \mathbf{A}^T - \mathbf{1} \end{bmatrix}, \quad \tilde{\mathbf{L}} := \begin{bmatrix} \mathbf{L} \\ \mathbf{I}_K \end{bmatrix}, \quad (34)$$

where \mathbf{A} is a $m \times K$ matrix with elements a_{jk} and \mathbf{I}_K is the $K \times K$ identity matrix. In other words, each of the K pseudodocuments is attributed entirely to a single topic, and the Dirichlet prior parameters are treated as “pseudocounts”.

Similarly, the Poisson NMF penalized loss function $\ell^*(\mathbf{H}, \mathbf{W})$ —in which minimizing this loss function corresponds to computing Poisson NMF MAP estimates (32)—can be rewritten in the form of the unpenalized Poisson NMF objective function, $\ell(\mathbf{X}; \mathbf{H}, \mathbf{W})$. To show this, we employ a change of variables that rescales the columns of \mathbf{H} and \mathbf{W} , $\mathbf{W}'\mathbf{U} \leftarrow \mathbf{W}$, $\mathbf{H}' \leftarrow \mathbf{H}\mathbf{U}$, where $\mathbf{U} := \text{diag}(\mathbf{u})$, and the columns of \mathbf{W}' are constrained to sum to one,

$\sum_{j=1}^m w'_{jk} = 1, k = 1, \dots, K$. With this change of variables, the penalized loss function can be rewritten as

$$\ell^*(\mathbf{X}; \mathbf{H}', \mathbf{W}') = \ell(\mathbf{X}; \mathbf{H}', \mathbf{W}') - \sum_{j=1}^m \sum_{k=1}^K (a_{jk} - 1) \log(u_k w'_{jk}) + \sum_{k=1}^K b_k u_k.$$

With this objective, one can independently solve for each u_k , with an analytic solution, $\hat{u}_k = \sum_{j=1}^m (a_{jk} - 1)/b_k$, that does not depend on the other parameters. Therefore, we focus on the part of the loss function that depends on \mathbf{H}', \mathbf{W}' , that is,

$$\ell^*(\mathbf{X}; \mathbf{H}', \mathbf{W}') = \ell(\mathbf{X}; \mathbf{H}', \mathbf{W}') - \sum_{j=1}^m \sum_{k=1}^K (a_{jk} - 1) \log w'_{jk} + \text{const},$$

where the “const” is a placeholder for terms that do not depend on \mathbf{H}' or \mathbf{W}' . This can be written as $\ell^*(\mathbf{X}; \mathbf{H}', \mathbf{W}') = \ell(\tilde{\mathbf{X}}; \tilde{\mathbf{H}}'; \mathbf{W}') + \text{const}$, where $\tilde{\mathbf{X}}$ is the data matrix augmented with pseudocounts (34), and $\tilde{\mathbf{H}}' := \begin{bmatrix} \mathbf{H}' \\ \mathbf{I}_K \end{bmatrix}$ is the matrix \mathbf{H}' augmented with pseudodocuments. Finally, we revert back to the original parameterization:

$$\tilde{\mathbf{H}}\hat{\mathbf{U}} \leftarrow \tilde{\mathbf{H}}', \quad \mathbf{W} \leftarrow \mathbf{W}'\hat{\mathbf{U}}.$$

where $\hat{\mathbf{U}} := \text{diag}(\hat{\mathbf{u}})$.

To summarize, this shows that MAP estimation (32, 33) can be reduced to MLE estimation (13, 14) when \mathbf{X} is replaced with $\tilde{\mathbf{X}}$, and \mathbf{H} is replaced with $\tilde{\mathbf{H}}$; that is,

$$\arg\max_{\mathbf{H}, \mathbf{W}} p_{\text{PNMF}}(\mathbf{X} \mid \mathbf{H}, \mathbf{W}) p_{\text{gamma}}(\mathbf{W}) = \arg\max_{\mathbf{H}, \mathbf{W}} p_{\text{PNMF}}(\tilde{\mathbf{X}} \mid \tilde{\mathbf{H}}, \mathbf{W})$$

and

$$\arg\max_{\mathbf{L}, \mathbf{F}} p_{\text{MTM}}(\mathbf{X} \mid \mathbf{L}, \mathbf{F}) p_{\text{dirichlet}}(\mathbf{F}) = \arg\max_{\mathbf{L}, \mathbf{F}} p_{\text{MTM}}(\tilde{\mathbf{X}} \mid \tilde{\mathbf{L}}, \mathbf{F}).$$

Therefore, we can apply Corollary 1 to prove Corollary 2. \square

A.2 EM Algorithms

A.2.1 EM for the Additive Poisson Regression Model

Here we rederive the basic EM algorithm [67, 71, 72] for fitting the additive Poisson regression model (23). To do so, we first introduce a data-augmented version of the Poisson regression model:

$$\begin{aligned} z_{ik} &\sim \text{Poisson}(a_{ik}b_k) \\ y_i &= \sum_{k=1}^K z_{ik}. \end{aligned} \tag{35}$$

Under this data-augmented model, the expected complete log-likelihood is

$$E[\log p(\mathbf{y}, \mathbf{z} \mid \mathbf{A}, \mathbf{b})] = \sum_{i=1}^n \sum_{k=1}^K \bar{z}_{ik} \log(a_{ik}b_k) - \sum_{i=1}^n \sum_{k=1}^K a_{ik}b_k + \text{const}, \tag{36}$$

where “const” includes additional terms in the likelihood that do not depend on \mathbf{b} , and $\bar{z}_{ik} = E[z_{ik}]$ is the expected value of z_{ik} with respect to the posterior $p(\mathbf{z} \mid \mathbf{A}, \mathbf{b}, \mathbf{y})$.

Using this data-augmented model, the M step (26) is derived by taking the partial derivative of (36) with respect to b_k , and solving for b_k . The E step (26) involves computing posterior expectations at the current $\mathbf{b} = (b_1, \dots, b_K)$. The posterior distribution of $z_i = (z_{i1}, \dots, z_{iK})$ is multinomial with y_i trials and multinomial probabilities $p_{ik} \propto a_{ik}b_k$. Therefore, the posterior expected value of z_{ik} is

$$\bar{z}_{ik} = y_i p_{ik} = y_i a_{ik} b_k / \mu_i. \quad (37)$$

The EM algorithm iterates the E and M steps until some stopping criterion is met. Alternatively, the E and M steps can be combined, yielding the update

$$b_k^{\text{new}} \leftarrow b_k \times \frac{\sum_{i=1}^n a_{ik} y_i / \mu_i}{\sum_{i=1}^n a_{ik}}. \quad (38)$$

A.2.2 Alternative EM Algorithm for Additive Poisson Regression

The additive Poisson regression model (23) is equivalent to a *multinomial mixture model* by a simple reparameterization. The multinomial mixture model is

$$\begin{aligned} y_1, \dots, y_n &\sim \text{Multinomial}(t, \boldsymbol{\pi}), \\ \pi_i &= \sum_{k=1}^K a'_{ik} b'_k, \end{aligned} \quad (39)$$

in which $\mathbf{A}' \in \mathbf{R}_+^{n \times K}$, $\mathbf{y} = (y_1, \dots, y_n) \in \mathbf{R}_+^n$, $\boldsymbol{\pi} = (\pi_1, \dots, \pi_n)$ and $t = \sum_{i=1}^n y_i$. To ensure that the π_i 's are probabilities, we require $b'_k \geq 0$, $a'_{ik} \geq 0$, $\sum_{k=1}^K b'_k = 1$, $\sum_{i=1}^n a'_{ik} = 1$. The multinomial mixture model is a reparameterization of the Poisson regression model (23) that preserves the likelihood; that is,

$$\prod_{i=1}^n \text{Poisson}(y_i; \mu_i) = \text{Multinomial}(\mathbf{y}; t, \boldsymbol{\pi}) \times \text{Poisson}(t; s), \quad (40)$$

in which the left-hand side quantities \mathbf{A}' , \mathbf{b}' , s are recovered from the left-hand side quantities \mathbf{A} , \mathbf{b} as follows:

$$\begin{aligned} u_k &\leftarrow \sum_{i=1}^n a_{ik} \\ a'_{ik} &\leftarrow a_{ik} / u_k \\ s &\leftarrow \sum_{k=1}^K b_k u_k \\ b'_k &\leftarrow b_k u_k / s. \end{aligned} \quad (41)$$

The EM algorithm for fitting the multinomial mixture model consists of iterating the following E and M steps:

$$p_{ik} = \frac{a'_{ik} b'_k}{\sum_{j=1}^K a'_{ij} b'_j} \quad (42)$$

$$b'_k = \frac{1}{t} \sum_{i=1}^n y_i p_{ik}. \quad (43)$$

Once the multinomial mixture model parameters b'_1, \dots, b'_K have been updated by performing one or more EM updates, the Poisson regression model parameters b_1, \dots, b_K are recovered as $b_k = t b'_k / u_k$, using the MLE of s , $s = t$.

A.2.3 Multiplicative Updates for Poisson NMF

Having derived EM for the additive Poisson regression model in the previous section, we can use this result to (re)derive the multiplicative updates for Poisson NMF [4] by making the following substitutions: making substitutions $\mathbf{A} \leftarrow \mathbf{W}$, $\mathbf{y} \leftarrow \mathbf{x}_i$, $\mathbf{b} \leftarrow \mathbf{h}_i$ in (38), where \mathbf{h}_i denotes a row of \mathbf{H} and \mathbf{x}_i denotes a row of \mathbf{X} , the update becomes the Poisson NMF multiplicative update for \mathbf{H} (27); similarly, making substitutions $\mathbf{A} \leftarrow \mathbf{H}$, $\mathbf{y} \leftarrow \mathbf{x}_j$, $\mathbf{b} \leftarrow \mathbf{w}_j$ in (38), where \mathbf{w}_j denotes a row of \mathbf{W} and \mathbf{x}_j denotes a column of \mathbf{X} , the update becomes the Poisson NMF multiplicative update for \mathbf{W} (28).

A.2.4 EM for the Multinomial Topic Model

Here we derive EM for the multinomial topic model [55], and connect EM for the multinomial topic model and the multiplicative updates for Poisson NMF. The EM algorithm for the multinomial topic model is based on a data-augmented version of the topic model [31],

$$\begin{aligned} p(z_{it} = k \mid \mathbf{L}) &= l_{ik} \\ p(d_{it} = j \mid \mathbf{F}, z_{it} = k) &= f_{jk}, \end{aligned} \quad (44)$$

where $d_{it} \in \{1, \dots, K\}$, and the data are $d_{it} \in \{1, \dots, m\}$, $t = 1, \dots, n_i$, in which n_i is the size of document i . Summing over the topic assignments z_{ij} recovers the multinomial topic model (5), in which the word counts are recovered as $x_{ij} = \sum_{t=1}^{n_i} \delta_j(d_{it})$.

The E step consists of computing the posterior expected values for the latent topic assignments z_{ij} ,

$$p_{ijk} := p(z_{ij} = k \mid \mathbf{X}, \mathbf{L}, \mathbf{F}) = l_{ik} f_{jk} / \pi_{ij}. \quad (45)$$

The M step for the topic proportions l_{ik} and word frequencies f_{jk} is

$$l_{ik} = \sum_{j=1}^m x_{ij} p_{ijk} / n_i \quad (46)$$

$$f_{jk} \propto \sum_{i=1}^n x_{ij} p_{ijk}. \quad (47)$$

Combining the E and M steps, we obtain the following updates:

$$l_{ik}^{\text{new}} \leftarrow \frac{l_{ik}}{t_i} \sum_{j=1}^m x_{ij} f_{jk} / \pi_{ij} \quad (48)$$

$$f_{jk}^{\text{new}} \leftarrow \frac{f_{jk}}{\xi_k} \sum_{i=1}^n x_{ij} l_{ik} / \pi_{ij}. \quad (49)$$

Here, $\xi_k > 0$ is a normalizing factor that ensures that $\sum_{j=1}^m f_{jk}^{\text{new}} = 1$. To connect to Poisson NMF, these updates can also be derived by applying PNMf-TO-MTM and its inverse to the Poisson NMF multiplicative updates (27, 28).

A.3 KKT Conditions

The first-order KKT conditions for the Poisson NMF optimization problem (2) are

$$\nabla_{\mathbf{H}} \mathcal{L}(\mathbf{X}; \mathbf{H}, \mathbf{W}, \mathbf{\Gamma}, \mathbf{\Omega}) = \mathbf{0} \quad (50)$$

$$\nabla_{\mathbf{W}} \mathcal{L}(\mathbf{X}; \mathbf{H}, \mathbf{W}, \mathbf{\Gamma}, \mathbf{\Omega}) = \mathbf{0} \quad (51)$$

$$\mathbf{\Gamma} \odot \mathbf{H} = \mathbf{0} \quad (52)$$

$$\mathbf{\Omega} \odot \mathbf{W} = \mathbf{0} \quad (53)$$

in which $\mathcal{L}(\mathbf{X}; \mathbf{H}, \mathbf{W}, \mathbf{\Gamma}, \mathbf{\Omega})$ denotes the Lagrangian function,

$$\mathcal{L}(\mathbf{X}; \mathbf{H}, \mathbf{W}, \mathbf{\Gamma}, \mathbf{\Omega}) := \ell(\mathbf{X}; \mathbf{H}, \mathbf{W}) - \|\mathbf{\Gamma} \odot \mathbf{H}\|_{1,1} - \|\mathbf{\Omega} \odot \mathbf{W}\|_{1,1}.$$

To define the Lagrangian function, we have introduced two matrices of Lagrange multipliers, $\mathbf{\Gamma} \in \mathbf{R}_+^{n \times K}$ and $\mathbf{\Omega} \in \mathbf{R}_+^{m \times K}$, associated with the non-negativity constraints $\mathbf{H} \geq \mathbf{0}$ and $\mathbf{W} \geq \mathbf{0}$. Combining (50) and (51), we obtain

$$\begin{aligned} \mathbf{\Omega} &= (1 - \mathbf{U})^T \mathbf{H} \\ \mathbf{\Gamma} &= (1 - \mathbf{U}) \mathbf{W}, \end{aligned} \quad (54)$$

in which \mathbf{U} is an $n \times m$ matrix with entries $u_{ij} = x_{ij} / \lambda_{ij}$. See also [6] and [7] for generalizations of these KKT conditions.

B Algorithm Implementation and Enhancements

B.1 Extrapolated Updates

To accelerate convergence of the EM and CD updates, we used the extrapolation method of [84]. In brief, at iteration t , the extrapolated update is

$$\begin{aligned} \mathbf{H}^{\text{ext}} &\leftarrow P_+[\mathbf{H}^{\text{new}} + \beta^{(t)}(\mathbf{H}^{\text{new}} - \mathbf{H}^{(t-1)})] \\ \mathbf{W}^{\text{ext}} &\leftarrow P_+[\mathbf{W}^{\text{new}} + \beta^{(t)}(\mathbf{W}^{\text{new}} - \mathbf{W}^{(t-1)})], \end{aligned} \quad (55)$$

where \mathbf{H}^{new} is a new estimate obtained by solving FIT-POIS-REG($\mathbf{W}^{(t-1)}, \mathbf{x}_i$) for each $i = 1, \dots, n$, \mathbf{W}^{new} is a new estimate obtained by FIT-POIS-REG($\mathbf{H}^{\text{ext}}, \mathbf{x}_j$) for each $j = 1, \dots, m$, $P_+(\mathbf{A})$ is the projection of matrix \mathbf{A} onto the non-negative orthant, $P_+(\mathbf{A})_{ij} := \max\{0, (\mathbf{A})_{ij}\}$, and $\beta^{(t)} \in [0, 1]$ is a parameter that interpolates between the updated estimate and the estimate from the previous iteration. (Note that setting $\beta^{(t)} = 0$ recovers the update with no extrapolation.)

Although [84] developed the extrapolation method for Frobenius-norm NMF, our initial trials showed that it also worked well for Poisson NMF. It also worked better than the other acceleration schemes we tried: the damped Anderson (DAAREM) method of [43] and the quasi-Newton acceleration method of [41].

B.2 Other Enhancements and Implementation Details

Here we detail other steps taken to speed up computation and improve numerical stability of the Poisson NMF optimization algorithms.

Computations with sparse data. Topic modeling data sets often have very high levels of sparsity; that is, most of the counts x_{ij} are zero. We therefore used sparse matrix computation techniques to reduce computational effort for sparse data sets. To illustrate the importance of sparse computations, consider computing the Poisson NMF loss function $\ell(\mathbf{X}; \mathbf{H}, \mathbf{W})$ when \mathbf{X} is sparse. Once the $\|\mathbf{H}\mathbf{W}^T\|_{1,1}$ term is computed, which requires $O((n+m)K)$ operations, computing $\phi(\mathbf{X}; \mathbf{H}, \mathbf{W})$ requires an additional $O(NK)$ operations, where N is the number of nonzeros in \mathbf{X} , because terms in the sum corresponding to $x_{ij} = 0$ can be ignored. Therefore, for sparse \mathbf{X} the time complexity of computing $\ell(\mathbf{X}; \mathbf{H}, \mathbf{W})$ is $O((N + n + m)K)$. Without considering sparsity, the time complexity is $O(nmK)$, which is much greater than $O((N + n + m)K)$ when $n \times m \gg N$. Similar logic applies to other computations such as gradients and EM (multiplicative) updates.

Incomplete optimization of subproblems. In practice, accurately solving each subproblem $\text{FIT-POIS-REG}(\mathbf{L}, \mathbf{x}_j)$ and $\text{FIT-POIS-REG}(\mathbf{F}, \mathbf{x}_i)$ may not be necessary, particularly in initial stages when \mathbf{H} and \mathbf{W} change a lot from one iteration to the next. Incompletely solving the subproblems has been shown to work well for Frobenius-norm NMF [47, 52, 94]. Therefore, instead of running the EM or CD algorithm to convergence, we stopped the optimization early when the number of iterations exceeded some limit. We found that performing at most 4 EM or CD updates worked well in practice when initialized to the estimate from the previous (outer-loop) iteration. We write this incomplete optimization as $\text{FIT-POIS-REG}(\mathbf{A}, \mathbf{y}, \mathbf{b}_0)$, where \mathbf{b}_0 makes explicit the dependence on an initial estimate. Therefore, when the subproblems are solved incompletely, $\text{FIT-POIS-REG}(\mathbf{W}^{(t-1)}, \mathbf{x}_i)$ is replaced with $\text{FIT-POIS-REG}(\mathbf{W}^{(t-1)}, \mathbf{x}_i, \mathbf{h}_i^{(t-1)})$ in Algorithm 1, and $\text{FIT-POIS-REG}(\mathbf{H}^{(t)}, \mathbf{x}_j)$ is replaced with $\text{FIT-POIS-REG}(\mathbf{H}^{(t)}, \mathbf{x}_j, \mathbf{w}_j^{(t-1)})$.

Parallel computations. We used Intel Threading Building Blocks (TBB) multithreading [95] to solve $\text{FIT-POIS-REG}(\mathbf{W}, \mathbf{x}_i)$, $i = 1, \dots, n$, and $\text{FIT-POIS-REG}(\mathbf{H}, \mathbf{x}_j)$, $j = 1, \dots, m$, in parallel.

Refinement of CD updates. Since the CD updates were performed without a line search, we found that the CD updates sometimes failed to improve the objective when the iterate was far away from a solution. Therefore, to reduce the failure rate of the CD updates, we performed a single EM update prior to running each CD update.

Improved convergence guarantees. Following [94], any parameter estimates that fell below 10^{-15} were set to this value.

Rescaled updates. To improve numerical stability of the updates, as others have done (e.g., [3]), we rescaled \mathbf{W} and \mathbf{H} after each full update. Specifically, we rescaled the matrices so that the column means of \mathbf{W} were equal to the column means of \mathbf{H} . Note that the Poisson rates $\lambda_{ij} = (\mathbf{H}\mathbf{W}^T)_{ij}$ and the Poisson NMF loss function $\ell(\mathbf{X}; \mathbf{H}, \mathbf{W})$ are invariant to this rescaling.

Assessing convergence. We used two measures to assess convergence of the iterates: (1) the change in the loss function $\ell(\mathbf{X}\mathbf{H}, \mathbf{W})$, which is the same as the change in the Poisson NMF log-likelihood; and (2) the maximum residual of the KKT conditions (Appendix A.3).

C Details of the Numerical Experiments

C.1 Data Sets

The NeurIPS [86] and newsgroups [87] data sets are word counts extracted from, respectively, 1988–2003 NeurIPS (formerly NIPS) papers and posts to 20 different newsgroups. The data sets were retrieved from <http://ai.stanford.edu/~gal/data.html> and <http://qwone.com/~jason/20Newsgroups>. Documents with fewer than 2 nonzero word counts were removed.

The MCF-7 data are RNA-sequencing read counts from human MCF-7 cells [81]. These data were downloaded from the Gene Expression Omnibus (GEO) website, accession GSE152749.

The epithelial airway and 68k PBMC data sets are UMI (unique molecular identifier) counts from single-cell RNA sequencing experiments in trachea epithelial cells in C57BL/6 mice [89] and in “unsorted” human peripheral blood mononuclear cells (PBMCs) [Fresh 68k PBMC Donor A] [90]. The epithelial airway data were downloaded from GEO, accession GSE103354. Specifically, we downloaded file `GSE103354_Trachea_droplet_UMIcounts.txt.gz`. Genes that were not expressed in any of the cells were removed. For the 68k PBMC data, we downloaded the “Gene/cell matrix (filtered)” `tar.gz` file for the Fresh 68k PBMCs (Donor A) data set from the 10x Genomics website (<https://www.10xgenomics.com/datasets>). Genes that were not expressed in any of the cells were removed.

All data sets except the MCF-7 data set were stored as sparse $n \times m$ count matrices \mathbf{X} , where n is the number of documents or cells, and m is the number of words or genes. The MCF-7 data were not sparse, they were stored as a dense matrix. The data processing scripts are provided in the Zenodo repository [82].

C.2 Computing Environment

All computations on real data sets were run in R 3.5.1 [96], linked to the OpenBLAS 0.2.19 optimized numerical libraries, on Linux machines (Scientific Linux 7.4) with Intel Xeon E5-2680v4 (“Broadwell”) processors. For running the Poisson NMF optimization algorithms, which included some multithreaded computations, 8 CPUs and as much as 16 GB of memory were used.

C.3 Source Code and Software

The methods described in this paper were implemented in the `fastTopics` R package. The main numerical results (other than the in-depth illustration with the MCF-7 data set) were generated using version 0.5-24 of the R package. The core optimization algorithms were developed in C++ and interfaced to R using `Rcpp` [97]. The CD updates were adapted from the C++ code included with NNLM R package, version 0.4-3 [48]. The Zenodo repository

[82] (see also <https://github.com/stephenslab/fastTopics-experiments/>) contains the code implementing the numerical experiments, and a workflowr website [98] for browsing the results.

D Additional Figures

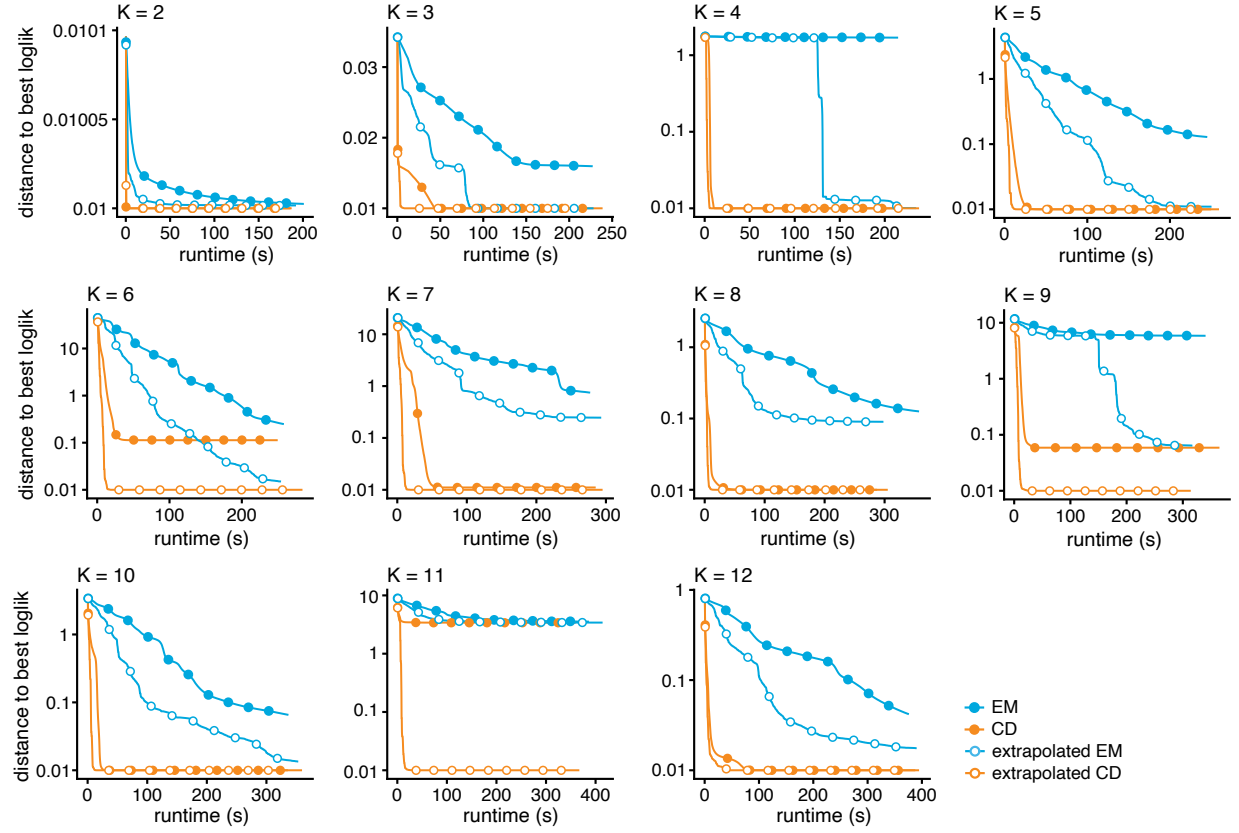


Figure 5: Improvement in model fit over time for the different Poisson NMF algorithms applied to the NeurIPS data. Multinomial topic model log-likelihoods are shown relative to the best log-likelihood recovered among the four algorithms compared (EM and CD, with and without extrapolation). Log-likelihood differences less than 0.01 are shown as 0.01. Circles are drawn at intervals of 100 iterations. Note that the 1,000 EM iterations performed during the initialization phase are not shown.

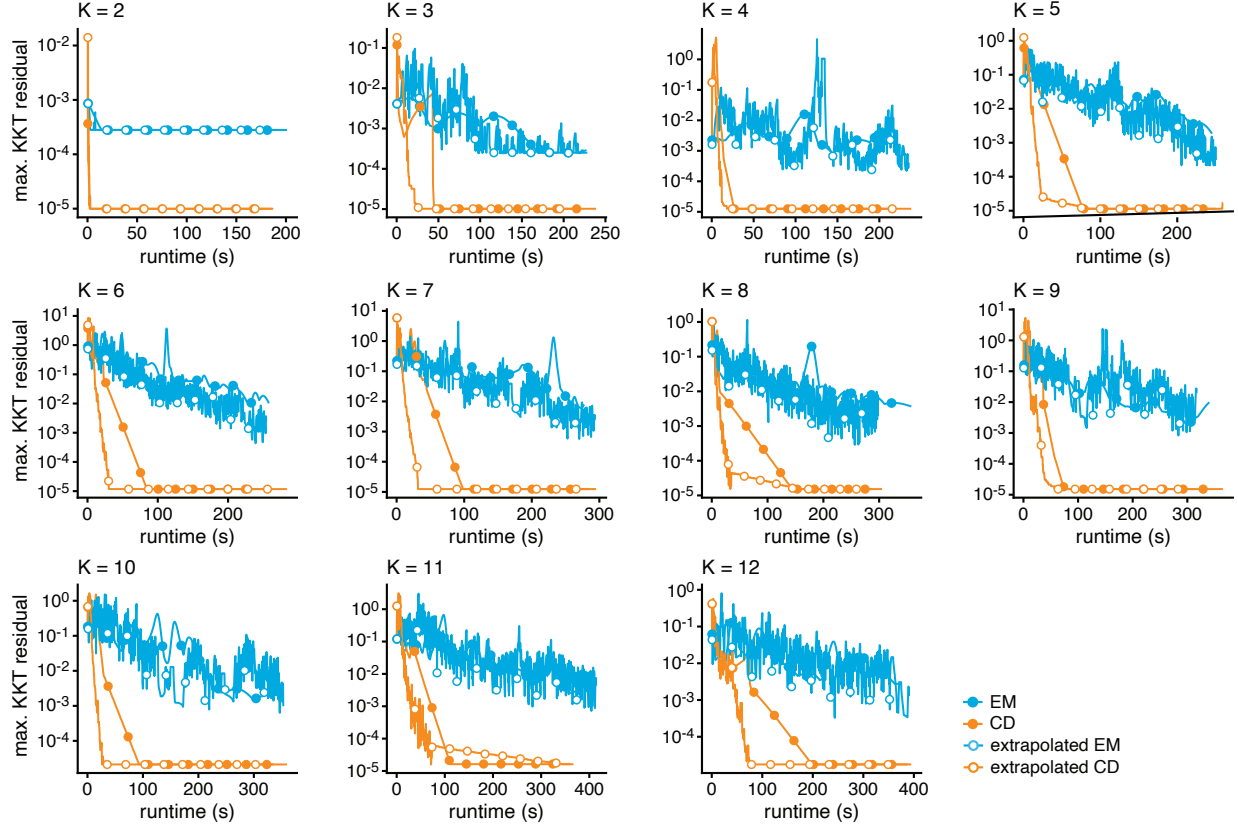


Figure 6: Evolution of the KKT residuals over time for the different Poisson NMF algorithms applied to the NeurIPS data. The KKT residuals should vanish near a local maximum of the Poisson NMF log-likelihood, so looking at the largest KKT residual can be used to assess how closely the algorithm recovers a stationary point (*i.e.*, an MLE). Note that the KKT residuals are not expected to decrease monotonically over time. Circles are drawn at intervals of 100 iterations.

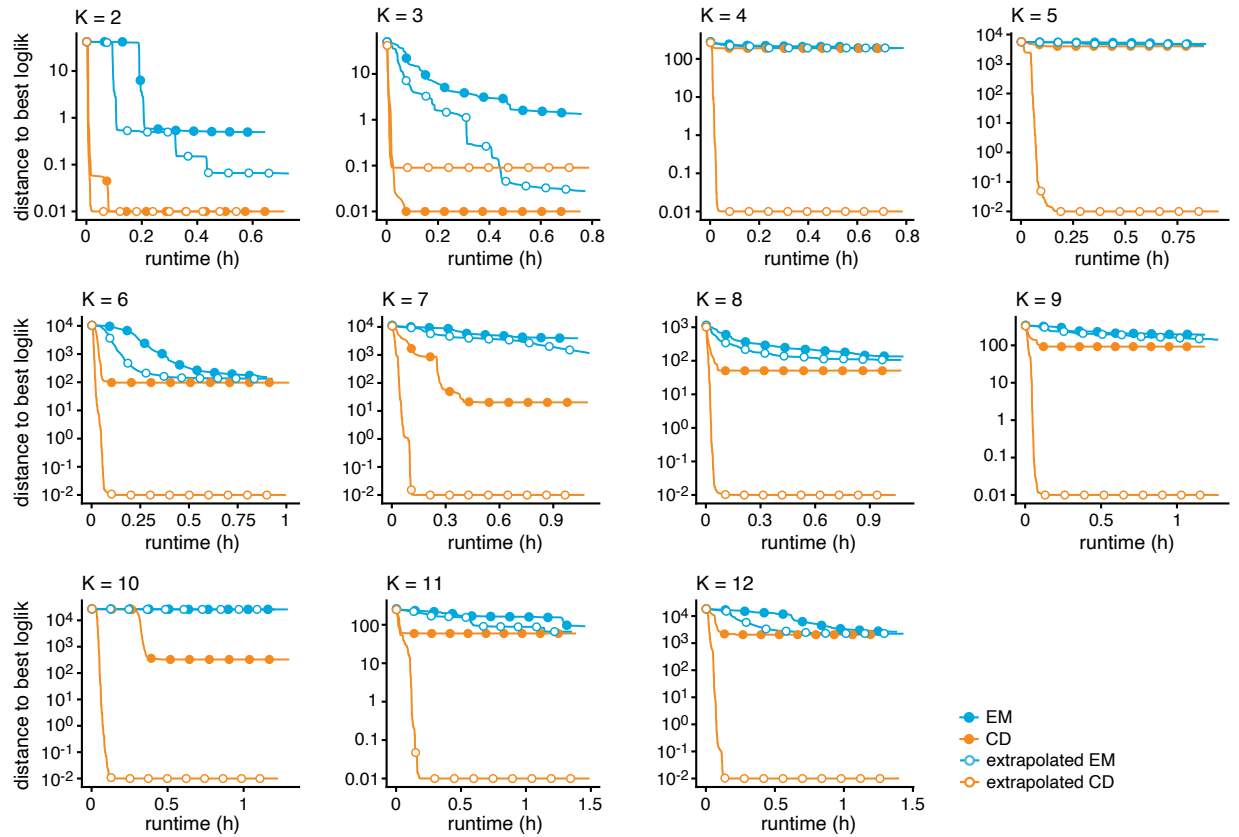


Figure 7: Improvement in model fit over time for the different Poisson NMF algorithms applied to the newsgroups data. See the Figure 5 caption for more details.

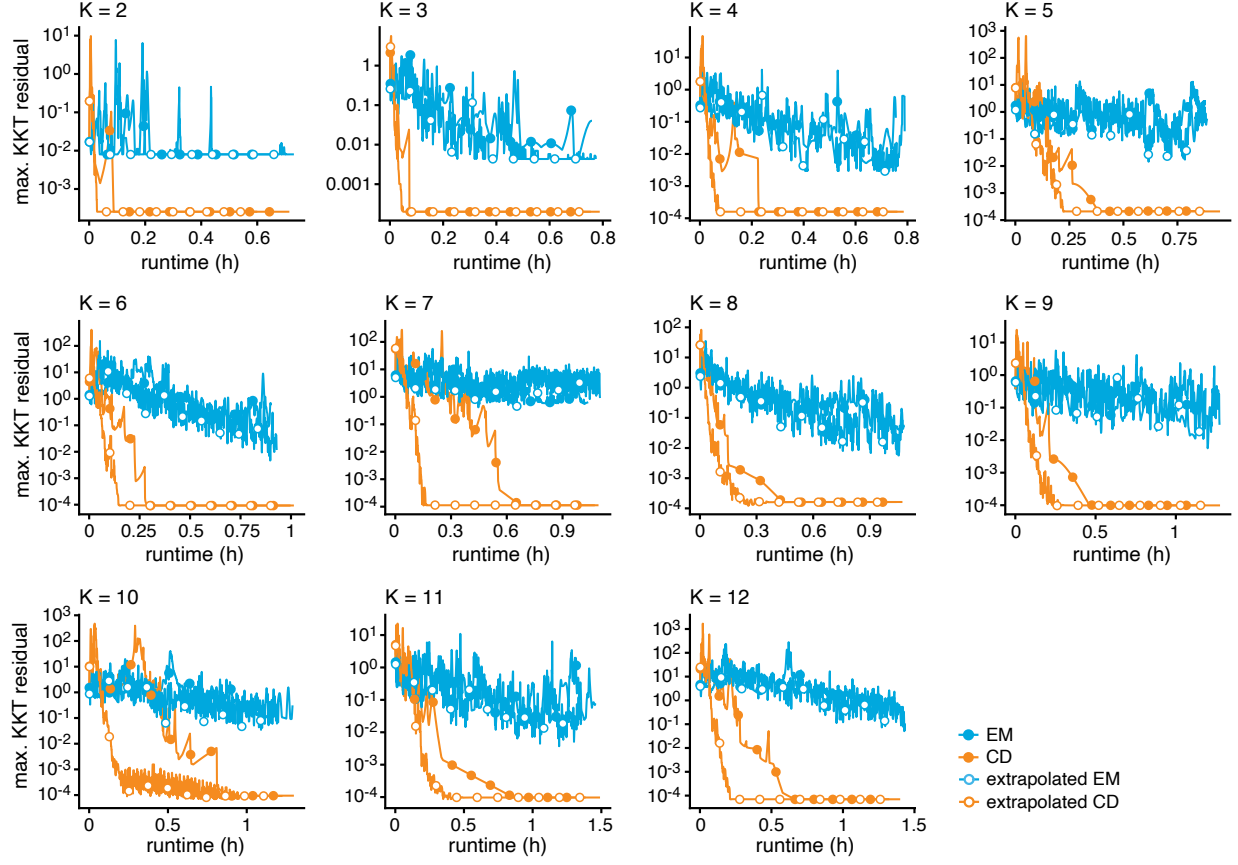


Figure 8: Evolution of the KKT residuals over time for the different Poisson NMF algorithms applied to the newsgroups data. See the Fig. 6 caption for more details.

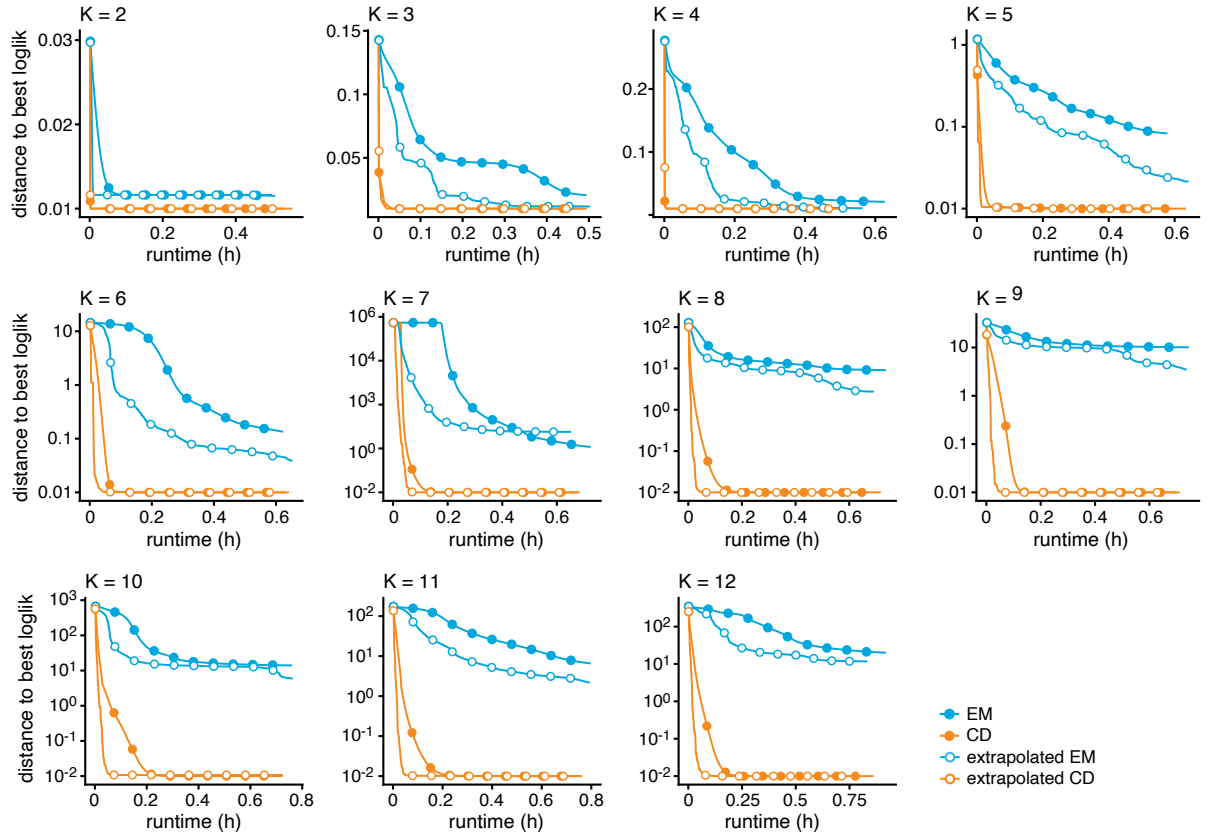


Figure 9: Improvement in model fit over time for the different Poisson NMF algorithms applied to the epithelial airway data. See the Figure 5 caption for more details.

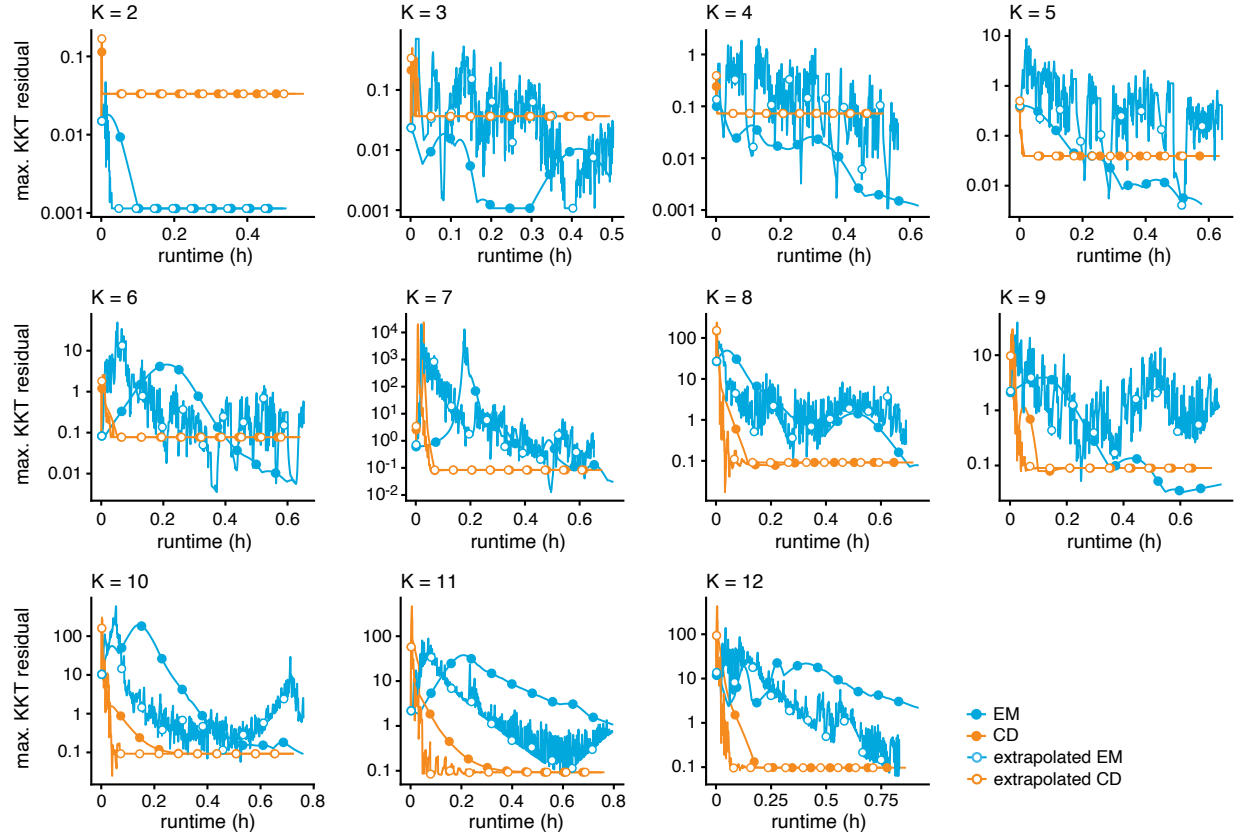


Figure 10: Evolution of the KKT residuals over time for the different Poisson NMF algorithms applied to the epithelial airway data. See the Figure 6 caption for more details.

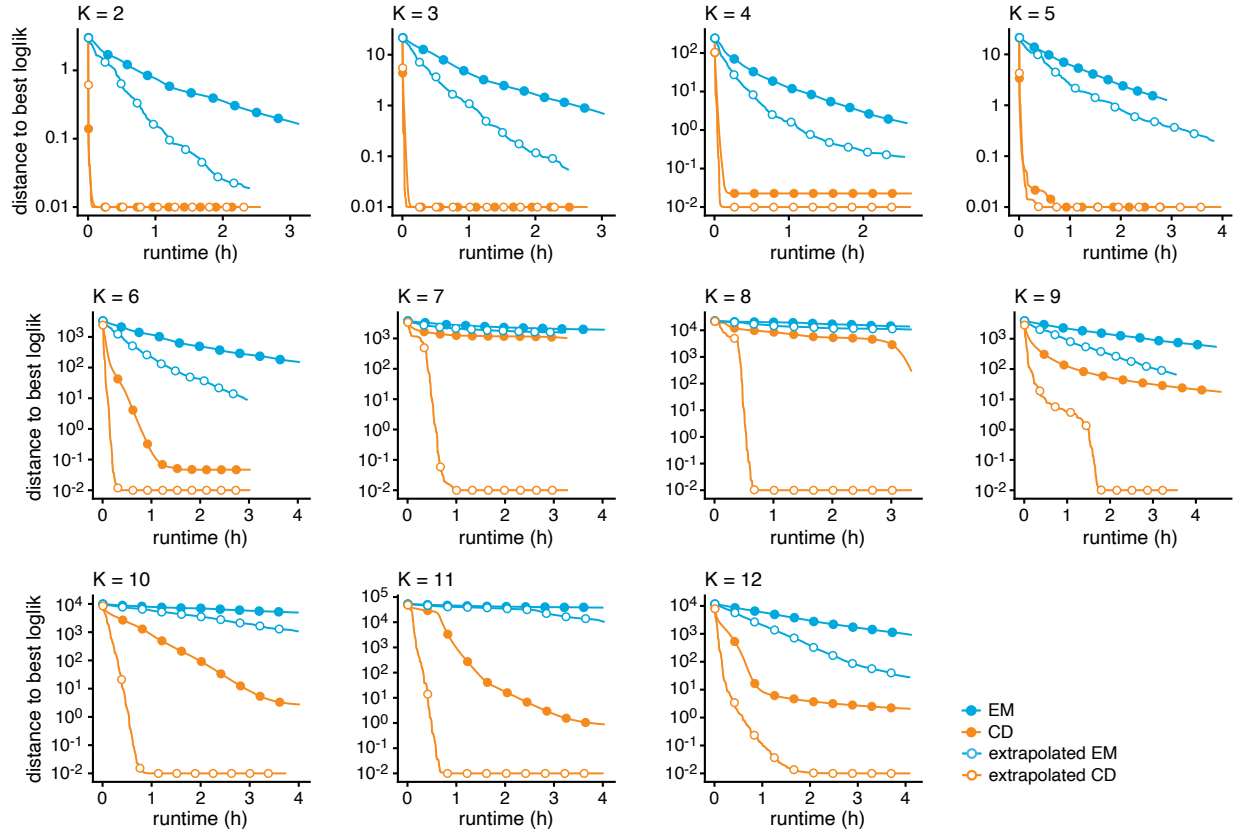


Figure 11: Improvement in model fit over time for the different Poisson NMF algorithms applied to the 68k PBMC data. See the Figure 5 caption for more details.

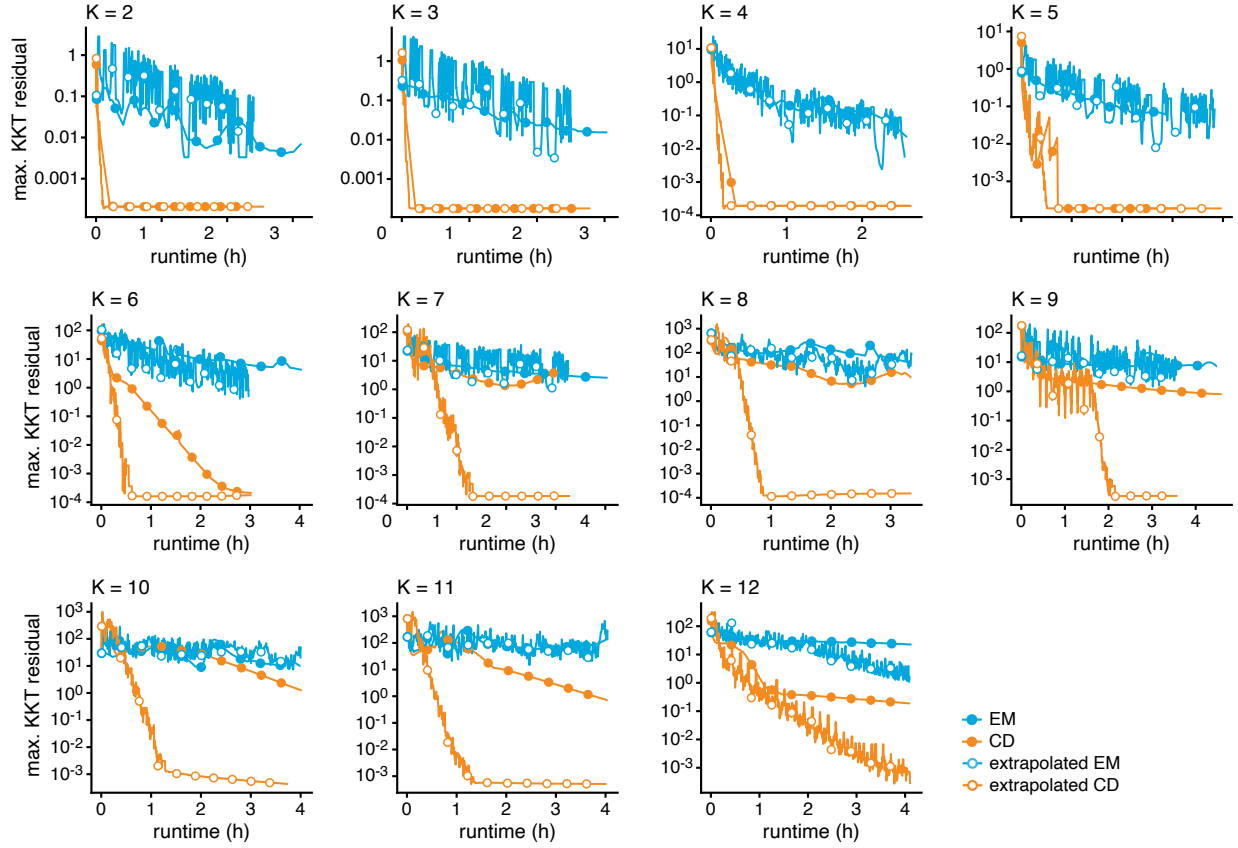


Figure 12: Evolution of the KKT residuals over time for the different Poisson NMF algorithms applied to the 68k PBMC data. See the Figure 6 caption for more details.